MEDICAL ROBOTS

Medical needles in the hands of AI: Advancing toward autonomous robotic navigation

Ron Alterovitz[1]*, Janine Hoelscher[2], Alan Kuntz[3]

Safely and accurately navigating needles percutaneously or endoscopically to sites deep within the body is essential for many medical procedures, from biopsies to localized drug deliveries to tumor ablations. The advent of image guidance decades ago gave physicians information about the patient's anatomy. We are now entering the era of AI (artificial intelligence) guidance, where AI can automatically analyze images, identify targets and obstacles, compute safe trajectories, and autonomously navigate a needle to a site with unprecedented accuracy and precision. We survey recent advances in the building blocks of AI guidance for medical needle deployment robots (perceiving anatomy, planning motions, perceiving instrument state, and performing motions) and discuss research opportunities to maximize the benefits of AI guidance for patient care.

INTRODUCTION

Reaching a specific site in the human body with a needle is a critical step in billions of medical procedures each year, making needles among the most widely used medical instruments (*1*–*7*). These procedures range from simple, routine tasks like vaccinations to complex procedures such as biopsies to diagnose cancer or other diseases, localized injections of drugs into tumors or other diseased tissues, percutaneous needle insertion to enable vascular access, brachytherapy to place radioactive seeds to locally kill tumors, and ablation to destroy diseased tissues. The success of the latter, more complex procedures, which collectively number in the millions of cases each year (*2*–*7*), depends on safely navigating a needle to a specific anatomical site with high accuracy.

Reaching a site with high accuracy using a needle is challenging. The needle's initial position and orientation and its path through tissue need to be determined and followed. The needle's path through tissue should avoid anatomical obstacles, including nonpenetrable structures such as bones as well as sensitive structures such as nerves, blood vessels, and other tissues, to which damage might result in negative side effects or procedure complications. Furthermore, tissues may move or deform because of needle/tissue interaction forces as well as physiological processes such as respiration and heartbeat. The needle can be deployed percutaneously (through the skin) or via an endoscope (for example, via a bronchoscope or colonoscope), raising additional navigation challenges.

Robots combined with artificial intelligence (AI) are showing promise in addressing these challenges and enabling needles to reach more targets safely and accurately. Robots provide greater accuracy and precision than physicians can achieve by manually guiding needles, and they also allow the use of advanced needle designs that can steer through the body. Advances in AI can improve procedure accuracy and safety as well as enable an increase in the level of automation of such procedures (*8*, *9*). AI can automatically analyze images, identify targets and obstacles, compute safe trajectories, and autonomously navigate an instrument to a site with unprecedented accuracy and precision.

[1]Department of Computer Science, University of North Carolina at Chapel Hill, Chapel Hill, NC 27599, USA. [2]Department of Bioengineering, Clemson University, Clemson, SC 29634, USA. [3]Kahlert School of Computing and Robotics Center, University of Utah, Salt Lake City, UT 84112, USA.
*Corresponding author. Email: ron@cs.unc.edu.

For decades, a dominant paradigm for accurately navigating instruments to a site within the human body has been image guidance. The field of image-guided interventions was set in motion in 1896, the year after x-rays were discovered, when physician John Hall-Edwards used an x-ray image of a patient's hand to surgically remove an embedded needle (*10*). The advent of computed tomography (CT) scans and magnetic resonance imaging (MRI) in the 1970s opened up more possibilities for interventional medical procedures: Physicians could see anatomy in three dimensions without surgically opening the patient. With preprocedure image guidance, physicians can visualize three-dimensional (3D) anatomy and plan needle paths before a procedure, enabling safer access to targets deep within the body than previously possible. In addition, with intraprocedure image guidance, physicians can adjust needle motions on the basis of feedback from imaging, further improving accuracy. One of the first medical robots to operate on a human used a needle and image guidance for a brain biopsy procedure in 1985 (*11*). In this pioneering work, image guidance enabled a physician, looking at a preoperative CT scan, to identify a tumor and plan a path for a needle biopsy. The physician then registered a robot to the CT image, and the robot automatically positioned and oriented a guide for a needle to accurately reach the target. Today, image guidance remains a dominant paradigm for achieving accurate needle placement.

Advances in AI are enabling a new form of procedure guidance: AI guidance. AI guidance leverages AI to enhance physician performance and create building blocks for higher levels of robot autonomy. The scope of AI methods relevant to AI guidance is quite broad. Since the term "artificial intelligence" was coined at a Dartmouth workshop in 1956, AI has expanded to cover a variety of techniques, including search algorithms, logical agents, probabilistic reasoning, learning (for which support vector machines and artificial neural networks are particular examples), natural language processing, and perception (*12*). For needle-based procedures, we consider the components of AI guidance to include perceiving anatomy, planning instrument motions, perceiving instrument state, and performing instrument motions during a procedure.

These AI guidance components can assist physicians or enable a medical robot to operate autonomously. Inspired by the levels of automation for self-driving vehicles standardized by the Society of Automotive Engineers (SAE) (*13*), five levels of automation have been defined for medical robots (*14*–*16*): robot assistance, task autonomy, conditional autonomy, high autonomy, and full automation (*14*). AI guidance components help a robot achieve a higher level of automation. The robot's automation level is limited by its AI guidance component that requires the most human involvement. For example, if planning motions is fully autonomous but performing those motions is done manually by the physician, the robot's level of automation is limited by the manual execution. Furthermore, AI guidance is enabling better procedure outcomes compared with traditional approaches, including in live humans (*17*, *18*) and ex vivo and in vivo animal studies (*19*, *20*). Advancements in AI guidance have the potential to further enhance physician performance and increase robot autonomy.

This article reviews the state of the art in AI guidance of medical needle deployment robots. We introduce the AI guidance components needed to enable higher levels of autonomy. We then review robots that percutaneously or endoscopically deploy needles to targets and discuss their AI guidance capabilities. We then discuss research opportunities to maximize the benefits of AI guidance for patient care.

AI GUIDANCE FOR NEEDLE-BASED PROCEDURES

We begin by defining the components of AI guidance for needle-based procedures (see Fig. 1). Each AI guidance component enhances procedure accuracy and safety, reduces physician effort, or increases the robot's level of automation. Each AI guidance component functions as a feature that physicians may find valuable and that medical robot vendors could promote as enhancing a robot's capabilities, ease of use, and clinical effectiveness.

The first AI guidance component is to perceive anatomy, which provides tools to understand the patient's anatomy, including the target to reach and anatomical obstacles to avoid. This can be achieved by acquiring and analyzing sensor data, such as medical images, camera images, 3D sensor data [e.g., RGB-D (red, green, blue, and depth) sensors, laser scanners, etc.], and force measurements, as well as other data sources such as image databases and patient medical record data. Key challenges include segmenting and identifying relevant anatomy in images and potentially fusing multiple sensor/data sources into a single comprehensive geometric or semantic understanding of the anatomy. This AI guidance component can be executed preprocedure (to facilitate preprocedure planning) or intraprocedure (to provide feedback during procedures). This AI guidance component can also be passive (analyzing provided sensor data) or active (guiding sensor data acquisition, for example, deciding when to activate fluoroscopy imaging, optimizing the view angle for an x-ray image, or selecting the parameters of an MRI scan).

The second AI guidance component is to plan motions, which involves computing safe, feasible motions that the medical instruments, such as needles and endoscopes, can follow to accomplish a procedure. The motions should be safe both inside the patient (for example, a needle should avoid damaging anatomical obstacles) and outside the patient (for example, the robot should safely avoid harming physicians and medical staff in the procedure room). This AI guidance component, like the one before, can be performed preprocedure (to plan a procedure before it starts) or intraprocedure (to plan the next steps of a procedure in progress). Planning motions can be direct or obstacle-avoiding, where the latter means that the medical instruments must avoid anatomical obstacles to ensure safety. Algorithms for this AI guidance component can be heuristic or optimal, where heuristic algorithms find feasible or good solutions and optimal algorithms guarantee optimization of clinically relevant criteria, such as minimizing procedure time, minimizing path length through tissue, or maximizing clearance from critical anatomical obstacles.

The third AI guidance component is to perceive instrument state, which involves understanding the state of the instruments, including the location and shape of instruments relative to perceived anatomy, as the procedure is in progress. Methods include state estimation, image analysis, sensor fusion, and registration methods between the patient, images, and instrument tracking sensors. The perceived instrument state can be partial (i.e., localizing only some part of the medical robot, such as the needle's tip) or complete (i.e., sensing the entire shape of the medical robot relative to the anatomy). Like the component of perceiving anatomy, this AI guidance component can also be passive and only analyze data provided to it or be active by acquiring images or moving the robot to better perceive the state of the instruments.

The fourth AI guidance component is to perform motions, which involves moving the instruments to accomplish a task. Methods include control integrated with motion planning and learning-based approaches that output controls. This component relies on the other AI guidance components to succeed. It can be static (i.e., the robot assumes that the anatomy is unchanging during the procedure) or adaptive (i.e., the robot updates its performance on the basis of real-time updates from other AI guidance components).

Each AI guidance component can evolve independently. For example, a robot that provides highly effective AI guidance for perceiving anatomy and perceiving instrument state has the potential to substantially accelerate and improve medical procedures, even if no AI guidance is provided for planning motions or performing motions. Thus, evaluating AI capabilities per component [Fig. 1 (top)] is useful. We illustrate the degree of AI guidance for any AI guidance component in Fig. 1 (bottom). This taxonomy is inspired by the Mobileye taxonomy for automated driving (*21*, *22*). Unlike SAE-inspired levels of automation (*14*) that apply to the whole robot, the Mobileye-inspired taxonomy can apply to individual AI guidance components.

The degree of AI guidance for a component reflects the physician's role, which decreases as AI guidance gains effectiveness. In the degree of full physician control, the physician performs the task without AI. In the degree of eyes-on/hands-on, the physician performs the task with AI providing assistance. For example, for the AI guidance component of perceiving anatomy, this might involve an image segmentation algorithm that requires a human to seed tissue types and make corrections. For performing motions, this degree of AI guidance might include virtual fixtures for needle control. In the degree of eyes-on/hands-off, the AI performs the task, and the physician monitors the AI and is prepared to intervene in unusual situations. For example, for perceiving anatomy, the AI might automatically segment an image, with a physician verifying correctness and making modifications in unusual situations. For performing motions, the AI could autonomously move the instruments under physician supervision. In the degree of eyes-off/hands-off, the AI performs the task and the physician only steps in when requested by the AI, which should only occur in unusual situations. In other words, the physician's role is to take action when the AI determines that it cannot complete its task autonomously. The final degree is full AI guidance, in which the AI performs the task. At this degree, the AI must be fully trusted to perform the task without supervision.

We next review the state of the art in medical needle deployment robots and then discuss their AI guidance components. We will

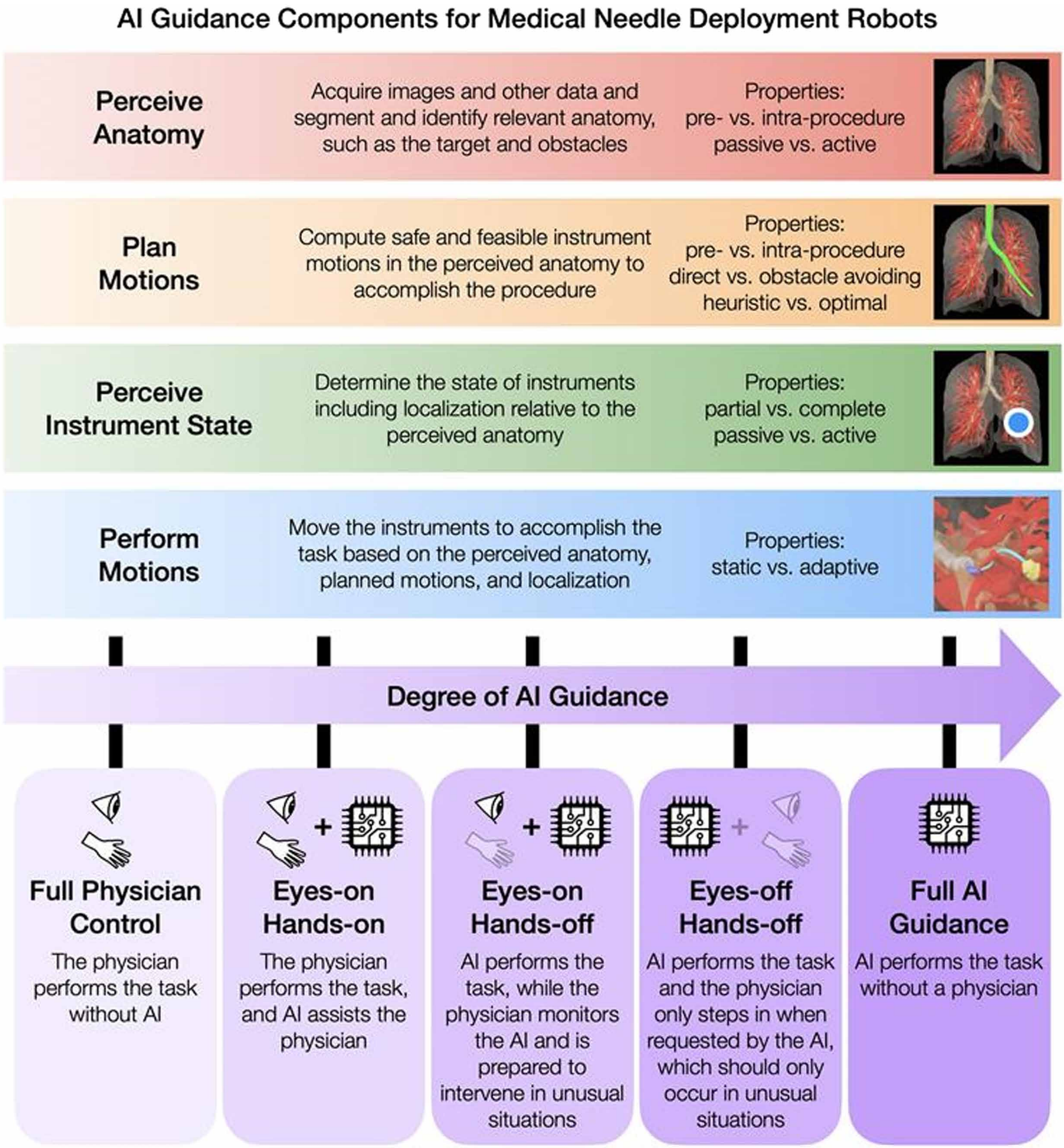

Fig. 1. AI guidance components for medical needle deployment robots. AI guidance components for needle-based procedures and the key properties of each component (top). The degree of AI guidance for a particular component can vary depending on the effort required by the physician. Each AI guidance component can be implemented to provide its own independent degree of AI guidance (bottom).

conclude with open research challenges for advancing AI guidance for needle-based procedures.

NEEDLE DEPLOYMENT ROBOTS AND THEIR APPLICATIONS

Medical needles, with their long history and varied applications, come in many forms. For this manuscript, we consider a medical needle to be a slender instrument that includes a rigid or flexible shaft with a pointed distal tip that moves through tissue (not fluid or air), with the shaft's proximal end starting outside the tissue and the distal portion following the tip as the tip moves through the tissue. Figure 2 shows different types of medical needles and their needle deployment methods. Needles can be straight (typically rigid and designed for straight paths through tissue) or steerable (capable of navigating along curved paths through tissue). Needles can also be deployed via direct insertion into the patient's tissues—either percutaneously (i.e., through the skin) or directly into a tissue type other than skin (for example, deploying a needle directly into the brain via a burr hole in the skull)—or via endoscopic insertion, in which case an endoscope (such as a bronchoscope or colonoscope) or related probe is used to deploy the needle into tissues. We next discuss medical robots that incorporate these various needle types and deployment approaches.

Straight needles require accurate positioning and orientation before insertion to accurately reach targets. Robots can assist by aligning the needle with the target. For robots with a low level of autonomy, assistance can take the form of a passive needle guide, similar in purpose to a stereotactic frame, which includes a tube or similar mechanism that helps align the needle before manual insertion. Robots have been developed to position and orient a needle guide to align the axis of a straight needle with a target (*11*, *18*, *23*–*33*). For higher levels of autonomy, the robot can also insert the straight needle after it is aligned with the target (*34*–*55*).

Straight-needle deployment robots have been applied to a variety of clinical applications. These applications include prostate biopsy and brachytherapy procedures (*26*, *56*, *57*), percutaneous vascular access (*28*, *45*, *50*, *53*, *54*, *58*–*60*), liver access for biopsy (*61*), breast biopsy (*62*), radiofrequency ablation (*51*), laser ablation (*23*), brain tumor biopsy (*11*, *49*), and ophthalmic procedures (*39*, *43*, *63*). Similar to straight needle insertion, rigid neuroendoscopes for transventricular access have been robotically inserted (*64*, *65*). Several straight-needle deployment robots have advanced to human testing, including systems with robotic needle guides (*11*, *24*, *25*) and with robotic needle deployment (*17*, *64*, *66*). Commercially available systems have included the Mona Lisa (*32*) and AmaKris (*33*) for prostate biopsy, ROSA (*30*) and Neuromate (*31*) for brain access, and Preceyes (*63*, *67*) for retinal insertion.

Steerable needles extend the capabilities of straight needles by enabling navigation along curved paths in tissue. Steering provides two important benefits: avoiding anatomical obstacles by curving around them to safely reach a target and correcting trajectory errors to improve accuracy without requiring pulling back the needle and reinserting. There are many types of steerable needles, but their unifying feature is that they can steer through tissue following curved paths (*68*–*71*).

Steerable needles can be steered using various mechanisms (*72*–*75*). Tip-steerable needles are a type of steerable needle for which the primary determinant of their ability to move along curves is a force and/or torque that is exerted onto the surrounding tissue at or near the needle's tip. Passive tip-steerable needles are tip-steerable needles for which the shape of the needle at or near its tip is not actively changed, and no energy is required for steering other than manipulations at the needle's base. Passive tip-steerable needles were inspired by the observation that many conventional medical needles bend when inserted into tissue because of their asymmetric, beveled tips. Some physicians learned to use this property to their advantage and made needles curve in a desired direction (*76*–*78*). On the basis of this idea, many different steerable needle designs have been developed.

Passive tip-steerable needles typically have asymmetric tips, such as bevels. When such a needle is inserted into tissue, the tissue exerts a force onto its tip, and the needle's asymmetric tip causes the needle to curve in the direction of the tip's asymmetry. Passive tip-steerable needles are inserted by axially translating the needle base, and they typically are steered by axially rotating the needle at its base, which changes the direction of the asymmetric tip. The curved paths achievable by this type of steerable needle can be modeled on the basis of the kinematics of a unicycle extended to three dimensions (*76*, *79*). Optimizing the design of the steerable needle's tip can increase the maximum curvature of the needle's paths, which consequently improves the needle's steerability, increasing the steerable needle's reachable workspace and the obstacles it can avoid. Bevel tips were proposed in early work, inspired by manually deployed clinical needles with bevels, which are used for a variety of applications, including brachytherapy and biopsies (*76*–*79*). Precurved or kinked tips increase the curvature of the needle but also create more tissue damage because the precurved tip cuts a helical pattern into the tissue when it is twisted (*80*, *81*). Flexure tips have a compliant bending point at which the needle bends during insertion but not during rotation, achieving similar curvatures but causing less tissue damage than precurved tips (*82*). Steerability can also be enhanced by tuning shaft stiffness using helical patterning on the needle shaft (*83*).

Active tip-steerable needles actively change the needle's shape at or near the tip to steer. Methods include extending and retracting a precurved stylet through the needle's main shaft (*84*), actuating tendons that bend the needle near its tip (*85*, *86*), using a push-pull mechanism consisting of two segments inside the needle (*87*), using an internal compliant mechanism (*88*), and using shape memory alloy actuators (*89*–*91*). Programmable bevel tips change the geometry of a needle's tip to create asymmetries, allowing steering in different directions (*92*). This can be achieved using two to four interlocking segments with bevels facing in different directions. Sliding the segments along one another in their axial direction changes the shape of the needle's tip in aggregate and, therefore, the direction and curvature of steering (*92*, *93*). Another approach uses directed tissue fracture to make room for the needle in the desired direction before inserting it (*94*, *95*).

Tip-steerable needles have been successfully tested in in vivo animal models. In vivo applications include drug delivery in the brain (*96*) and lung biopsy (*19*, *20*).

Base-steerable needles rely on manipulation of the needle at its base to bend the needle and deform tissue, causing the needle to move along curved trajectories. For example, the base of the needle can be translated transverse to its axis, which will deform the tissue and consequently reorient the tip of the needle inside the deformed tissue. By predicting using models or data the interaction of the needle with the surrounding deformable tissue, motion planners and controllers can compute needle base manipulations that steer the needle

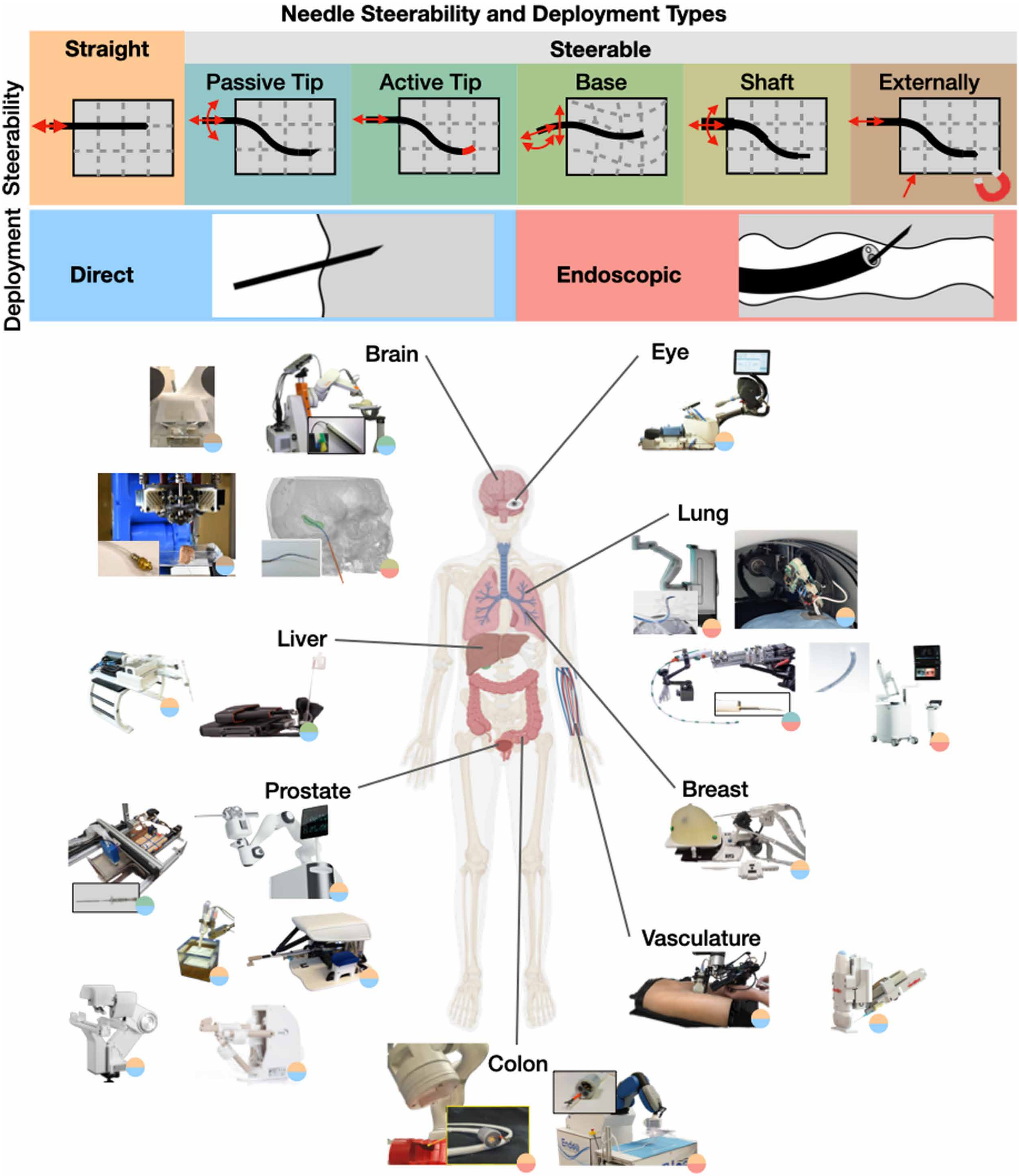

Fig. 2. Needle deployment robots can be classified on the basis of steerability type and deployment type. At the top, we illustrate needles in black, tissues in gray, and controllable elements (after entering tissue) in red. Below, we highlight needle deployment robots with different anatomical applications and classify them by their steerability type (top half of circle icons) and deployment type (bottom half). Anatomical applications include the eye (*63*), lung (*20*, *128*, *131*, *247*), breast (*34*), vasculature (*58*, *59*), colon (*120*, *121*), prostate (*140*, *189*, *248*–*251*), liver (*23*, *252*), and brain (*96*, *100*, *111*, *113*). Figure created with Biorender.com.

around obstacles and reach targets (*19*, *97*, *98*). This needle-steering approach was successfully tested in an in vivo animal model for prostate procedures (*19*), and a variant was commercialized and received US Food and Drug Administration approval (*99*).

Shaft-steerable needles leverage precurvature of the needle's shaft to enable steering. The most basic example is a needle that is precurved in a single planar arc. A more complex precurvature is a 3D helical shape (*100*). Concentric tube robots consist of multiple nested, precurved tubes that can each be independently extended and retracted as well as axially rotated to determine the shape of the robot. Concentric tube robots can operate in free space as general continuum manipulators. They can also be used as steerable needles, particularly if their design and controller allow for follow-the-leader deployment (*69*, *71*, *101*–*107*). Follow-the-leader (*108*) deployment ensures that the concentric tube robot's shaft follows the path of the tip through tissue, which prevents lateral tissue deformations or damage and allows concentric tube robots to be used safely and effectively as steerable needles inside tissue.

Externally steerable needles achieve curvature in tissue via forces and torques applied from outside the needle. One approach is leveraging magnetic actuation (*109*), including pulling the needle tip magnetically (*110*), pushing the needle while adjusting tip deflection with external magnets (*111*, *112*), and combining base rotation and a screw tip to pull the needle forward while steering with a magnet (*113*). Tip tendon actuation and magnetic steering can be combined to increase tip bending (*114*). Another approach is to deform tissue via external manipulation to push obstacles out of the way or push the target into the path of the needle (*115*). This approach is the inverse of other steering approaches; rather than curving the needle to avoid obstacles, the tissue is deformed so that the obstacles avoid the needle, and the target enters the needle's path. External steering approaches can be combined with other steering mechanisms to enhance steerability (*115*).

Beyond direct insertion, needles can also be deployed via endoscopes. Endoscopes navigate through open-air spaces inside the body, such as the airways or the digestive tract. We focus on endoscopes whose structure creates a continuous path from outside the patient to their tip inside the patient and are explicitly capable of deploying a needle. Such endoscopes can be rigid or flexible. Flexible robotic endoscopes can be steered using a variety of methods, including via a single actuated section near the distal tip that can bend in one (*116*) or multiple (*117*) directions, multiple tendon-driven sections (*118*, *119*), or an external magnet (*120*–*123*). Besides these robots that allow for the deployment of straight needles, steerable needles can also be deployed from endoscopes to further increase reachability (*20*, *124*, *125*). Applications for needle-deploying robotic endoscopes include bronchoscopies (*116*, *117*), colonoscopies (*118*, *120*–*123*), and brain access for biopsies (*119*). A magnetic colonoscopy robot with an instrument channel has recently advanced to clinical trials (*126*). Several endoscopic robots are commercially available today (*127*, *128*).

METHODS FOR AI GUIDANCE AND AUTOMATION

We next review methods developed to implement each AI guidance component for medical needle deployment robots. The software implementing the AI guidance components can run on computer hardware that is integrated with or attached to the robot [for example, the plan motions, perceive instrument state, and perform motions components in (*20*)] or on a remote computer or cloud-based service that exchanges data with the robot [for example, the perceive anatomy component in (*20*)].

Perceive anatomy

Medical needle deployment robots must understand the anatomical environment in which they operate, including the target to reach and anatomical obstacles to avoid. Going beyond basic image guidance that displays images, AI guidance for perceiving anatomy aims to gain a geometric or semantic understanding of the relevant anatomy to support a procedure. To perceive anatomy, AI can use a variety of data sources, particularly medical images from modalities such as ultrasound, CT, MRI, and RGB cameras. Robots with AI can also assist with image acquisition (*129*).

Traditionally, physicians manually analyze and annotate medical images, which can be tedious and imprecise. Early work on perceiving anatomy in images aimed for eyes-on/hands-on AI guidance by requiring a user to manually provide some information, like selecting seed points to initiate image segmentation on the basis of region growing or active surface methods (*130*). Recent approaches in medical image analysis focus on eyes-on/hands-off or higher degrees of AI guidance.

Preprocedure perception of anatomy often uses imaging modalities such as CT or MRI that provide 3D volumetric images. Needle deployment robots can use automatically segmented images for procedure planning [for example, (*131*–*133*)], and automatic image segmentation methods are integrated into commercial robots (*127*, *128*). With the advent of deep learning, a myriad of new techniques for medical image segmentation are being developed (*134*, *135*), which can be leveraged by medical robots.

Intraprocedure perception of anatomy can monitor changes in anatomy (and localize instruments relative to anatomy, which is covered under the AI guidance component of perceiving instrument state discussed later). Intraprocedure image analysis is often time critical and requires real-time performance. For intraprocedure MRI and CT imaging, the robot must fit and operate within the scanner bore (*37*, *38*, *46*, *51*, *131*). Leveraging intraprocedure MRI is further complicated given that conductive, metallic, and magnetic materials, including electric motors, cannot be used inside an MRI scanner because of its strong magnetic field (*136*). To address this challenge, MRI-conditional and MRI-safe needle deployment robots have been developed (*18*, *19*, *23*, *34*, *40*–*42*, *48*, *55*–*57*, *137*–*139*). Ultrasound imaging, with its lower overhead compared with CT and MR imaging, is widely used by needle deployment robots (*17*, *26*, *27*, *45*, *58*, *140*–*142*). Deep learning has enabled effective segmentation of ultrasound images (*53*, *59*, *143*). Intraprocedure ultrasound images can also be fused with other sensing modalities to account for deformation and motion (*26*, *144*) and enable more accurate intraprocedure vessel detection (*145*). Robots can automatically move ultrasound probes, enabling active perception of anatomy (*62*). Active techniques have also been developed for x-ray imaging (*146*).

For endoscopically deployed needles, intraprocedure endoscopic RGB camera images can be used for learning-based 3D anatomy reconstruction. Methods exist for bronchoscopies (*147*, *148*), ventriculoscopies (*149*), and colonoscopies (*150*).

Plan motions

Planning motions for a needle-based procedure, often referred to as procedure or image-guided planning, involves selecting a feasible path for the needle that reaches the target and avoids obstacles. Going beyond basic image-guided planning in which physicians use images to plan procedures, AI guidance for planning motions automates part or all of the planning process. We first review eyes-on/hands-off or higher degrees of AI guidance for planning motions, followed by eyes-on/hands-on AI guidance that incorporates physician feedback into the planning process.

For straight needles, planning motions requires determining a start pose for the needle and an insertion distance (*151*, *152*). Multitarget applications can optimize the start pose to reach multiple targets per insertion (*26*, *140*). Planning algorithms can also explicitly consider the impact of tissue deformations (*153*). Planning algorithms for straight needles can provide anatomical obstacle avoidance by adjusting the needle's start pose (*131*, *154*–*156*). Planning algorithms can also include collision avoidance for the robot arm deploying the needle (*131*, *157*).

Steerable needles can safely and accurately reach more targets because of their ability to move along curved paths in tissue and allow obstacle avoidance. However, these benefits come with the cost of increased planning complexity because more options need to be considered while adhering to the needle's kinematic constraints.

A variety of motion planners have been developed specifically for tip-steerable needles. Early motion-planning algorithms considered needle kinematics and tissue deformation or motion uncertainty but often assumed deployment in a 2D plane (*77*, *158*–*160*). Achieving the full potential of steerable needles requires planning in 3D, which is more complex. An early 3D planning approach used a diffusion method, but it did not consider obstacles (*161*). Optimization-based planning techniques iteratively improve plans on the basis of cost functions and can include obstacle avoidance (*162*–*164*). Sampling-based motion planners efficiently explore high-dimensional spaces and have been successfully applied to steerable needles (*20*, *165*–*170*). They can be combined with evolutionary optimization to refine plans (*171*). Inverse reinforcement learning has been applied to steerable needle motion planning (*172*). Needle planning methods have also been developed that explicitly consider tissue deformations by modeling needle/tissue interactions (*77*, *133*, *173*). Search-based planning methods systematically explore the needle's reachable workspace to find motion plans. A fractal tree approach (*174*, *175*) smooths candidate plans from a search tree to comply with the needle's hardware constraints. A search-based planner using appropriately selected needle motion primitives, under certain assumptions, guarantees both completeness and optimality (*176*).

Motion planners for tip-steerable needles typically compute 3D space curves from an insertion pose to a target, avoiding obstacles and respecting curvature constraints. These methods can apply to other steerable needle types that follow similar space curves. This includes some magnetically actuated externally steerable needles and some shaft-steerable needles. Customizations may be required. For example, for magnetically actuated externally steerable needles, the achievable curvature varies with the needle tip's distance from the external magnet (*113*).

For base-steerable needles, simulating tissue deformations is critical. Early planning algorithms modeled the needle's movement in 2D deformable tissue (*97*, *177*). Motion planning for externally steerable needles via tissue manipulation also requires modeling tissue deformation to compute manipulations that push obstacles out of the needle's path (*115*).

For shaft-steerable needles, planning motions can support not only computing paths to a target but also optimizing the design of the needle's constituent parts to enhance reachability. For helical needles, this includes optimizing the needle's curvature parameters (*100*). For concentric tube robots, this can involve specifying or optimizing the properties of the multiple tubes of the robot and determining a deployment strategy for those tubes (*69*, *71*, *101*–*107*, *178*–*182*). Planning methods that optimize tube designs are necessarily preprocedure. As mentioned previously, follow-the-leader (*108*) deployment is important when steering concentric tube robots through tissue. Early work on concentric tube robots often assumed dominating stiffness in the robot's outer tube(s), which ensures follow-the-leader motion when inner tubes are extended beyond the tip of the stiffer tubes, whereas recent work considers more realistic physics-based models of tube interactions. Many concentric tube robots with follow-the-leader designs have been developed for navigating tortuous and constrained anatomical passageways, such as vasculature, which is beyond this article's scope.

Many needle motion planners assume a fixed needle start pose. However, in practice, needles are often deployed from a surface (for example, skin), allowing multiple potential start poses. One approach is for the motion planner to consider many possible start poses and compute which one results in the best motion plan (*124*, *155*). Dynamic programming has been shown in a 2D setting to determine the position and orientation on an insertion surface that yields the highest probability of success (*160*). Another strategy is to invert the planning problem by planning backward from a target position toward an insertion surface (*183*, *184*).

Motion-planning algorithms for bronchoscopes navigating airways in the lung have been proposed (*124*, *185*, *186*). Bronchoscope motion is restricted by the airway tree structure, which simplifies the planning problem.

For eyes-on/hands-on AI guidance for planning motions, methods have been developed that incorporate physician input. Strategies include allowing physicians to select a start pose (*187*), draw an initial motion plan that is then optimized (*164*), and provide demonstrations for learning expert preferences (*187*).

Perceive instrument state

Conceptually related to perceiving anatomy is perceiving instrument state, involving understanding the location of relevant points on the needle and other system components relative to the perceived anatomy as well as other potentially relevant state information like instrument/tissue interaction forces. Perceiving instrument state enables closed-loop control, intraprocedure replanning, and verifying needle placement. Beyond basic image guidance where instrument state is read from sensors and can be registered to images, AI guidance can augment incomplete sensor data, reduce noise, and fuse sensing modalities. The appropriate degree of AI guidance is informed by, or often dictated by, the specific use of perceived instrument state. For example, if needle tip localization is being used by an automated motor control method, then eyes-off/hands-off may be the lowest AI guidance degree that is feasible for perceiving instrument state if the control method's execution frequency is too high to allow a human to effectively monitor and intervene with the localization method. As such, AI guidance approaches to perceiving instrument state predominately end up taking a hands-off approach, falling into the category of eyes-off/hands-off for most methods detailed below.

Historically, many approaches for localizing needles have been distinct from AI methods. Commonly, sensors are added to the system, and methods register sensor measurements to preprocedure or intraprocedure imaging of the anatomy (*188*). Examples include optical tracking markers affixed to the proximal end of rigid instruments or guiding frames, magnetic tracking coils embedded in the tips of steerable needles or endoscopes, and fiber Bragg grating fiber optic–based shape sensors (*19*, *85*, *189–191*). Other sensing modalities have been proposed to determine the state of a needle during insertion, including force sensors (*60*, *170*, *192*) and time-of-flight cameras to record needle insertion depth (*26*). Many robots have proprioceptive capabilities similar to those of humans via the use of motor and joint encoders and a computational understanding of the robot's mechanics; i.e., by knowing the state of the robot's joints, and the robot's geometry as a function of joint state, we can potentially infer the state of any instruments being held by or affixed to the robot. Such sensor- and proprioception-based methods are often effective but have limitations. These limitations include sensor noise and the difficulty in some cases of sensing all relevant degrees of freedom (DOFs). These challenges are exacerbated by the variety of curves that steerable needles can take and the clinical desire for needles with thin outer diameters, which restrict space available for onboard sensors, thus motivating AI guidance.

AI guidance–enhanced localization often combines this sensor data with observer models to estimate full instrument state. For instance, Kalman filters (*193*) (often extended Kalman filters, or EKFs) have been used to infer needle orientation from partial 2D (*194*, *195*) or 3D position data (*196*, *197*). Missing DOFs, such as roll in 5-DOF electromagnetic sensors (necessitated because of size requirements), have been estimated using deep recurrent networks (*198*) and torsion-aware EKFs (*199*).

AI guidance leveraging medical imaging methods for needle localization includes passive approaches using fluoroscopy (*98*) or MRI (*200–202*) and active methods such as robotically actuated ultrasound probes (*203*, *204*), needle vibration in ultrasound for better localization (*205*), MRI signal modulation (*41*, *42*), and optimal x-ray view planning (*146*, *206*). Needle guide and fiducial segmentation in MRI have also been combined with robot kinematics (*23*, *34*, *46*, *131*).

In endoscopy, tip cameras provide rich visual data. AI guidance can analyze these data to estimate endoscope location and orientation in anatomy (*117*, *207*, *208*).

Perform motions

Performing motions involves moving instruments during a procedure to accomplish the task. Going beyond basic image guidance that can display instrument motions relative to images, AI guidance for performing motions can partially or fully autonomously move instruments during a procedure. AI guidance is not required for performing motions during needle procedures. For example, straight needles and even steerable needles in certain circumstances can be deployed manually by physicians (*84*, *88*). However, steering needles in a 3D environment is not intuitive for human operators (*209*), making some degree of AI guidance critical for the adoption of these needle types. Furthermore, AI guidance for performing motions can improve the accuracy and safety of many needle procedures. Some methods for performing motions, particularly those based on control theory, evolved independently from the topics explored by the AI research community (*12*). We first review eyes-on/hands-on AI guidance for performing motions of needle-based procedures and then eyes-on/hands-off and higher degrees of AI guidance.

Eyes-on/hands-on AI guidance for performing motions requires human/AI collaboration to deploy a needle. As discussed earlier, a common method is for a robotic needle guide to assist in positioning and orienting a straight needle, and a human manually inserts the needle. Robotic needle guides can be remotely controlled (*18*) or move autonomously (*26*, *140*) to support planned needle trajectories.

Another approach to eyes-on/hands-on AI guidance is teleoperation, where the physician conceptually has hands-on control of the needle's motion by remotely controlling the needle deployment robot. In procedures with teleoperated devices, the physician provides control input, which the robot maps to low-level motor commands. Graphical user interfaces can support needle robot teleoperation via keyboard and mouse (*58*, *210*). Haptic devices may provide more intuitive interfaces for robot control inputs, including joystick-like devices (*35*, *117*, *127*, *211*, *212*), pen-like haptic devices (*47*, *142*, *209*, *213–218*), the Intuitive Surgical da Vinci Master Tool Manipulator (*219*), or custom devices representing the robot's DOFs (*38*, *43*, *128*, *137*, *220*). Teleoperating a robot requires situational awareness, typically through a visual interface showing the needle's current location with respect to anatomy. Beyond visual cues on a screen, head-mounted displays can enable augmented reality and support robot control via hand gestures (*221*). Other types of user feedback can be provided, including force feedback (*38*, *209*, *218*) and vibrotactile feedback (*142*). Teleoperation has been demonstrated for a tip-steerable needle in living brain tissue (*96*) and has been commercialized for a base-steerable needle (*99*). Performing motions for the magnetically actuated externally steerable needles requires controlling the motion of the external magnet that applies steering forces or torques to the needle tip. This can be done via teleoperation, where the user selects a desired steering direction and the magnet automatically moves to achieve the desired steering direction (*113*), or visually to compute currents for an array of enclosing electromagnets (*110*).

Eyes-on/hands-off AI guidance reduces the responsibility of the physician to simply monitoring the needle deployment. This degree of AI guidance has been achieved for straight-needle robots by actuating insertion of the needle to the target (*34*, *42*, *44*, *46*, *131*).

Achieving eyes-on/hands-off and higher degrees of AI guidance for steerable needles requires developing control algorithms for needle deployment. For tip-steerable needles, controlling motion along a curved path requires controlling its asymmetric tip. Early bevel-tip steerable needles were steered along paths composed of arcs corresponding to the needle's maximum curvature, where the plane of each arc was determined by axially rotating the needle tip to orient its bevel. The duty cycling technique rapidly switches between insertion with uniform axial rotation (steering straight) and insertion without rotation (steering curved) and thereby achieves needle-steering paths with varied curvatures (*80*). Further advances in needle control include a sliding mode controller (*222*) and a pause-and-go method (*20*) that takes a deadband-aware Kalman filter (*199*) approach to ensure that unknown needle torsion is minimized during control. These controllers can be used to follow motion plans computed using the AI guidance methods described in the Plan motions section. Another approach is to use fast replanning during deployment, which can be used to handle uncertainty or deviations, effectively serving as a controller and introducing adaptive properties to this component of

AI guidance (*145*, *204*, *223–226*). Steerable needle motion planners can also consider uncertainty and create a policy that is robust to deviations during robot deployment (*160*, *169*, *227*). Hands-off AI guidance using closed-loop control has also been demonstrated for active tip-steerable needles using electromagnetic localization (*212*) and for base-steerable needles using fluoroscopic image guidance (*98*). Eyes-on/hands-off AI guidance has been demonstrated in living tissue (*20*).

For shaft-steerable needles, performing motions can take an open-loop approach, given that these needles, particularly follow-the-leader concentric tube robots, are designed to accurately perform the planned motion (*100*, *178*, *179*, *181*). Closed-loop approaches can leverage intraprocedure control to follow the desired follow-the-leader trajectories without the need to customize the robot to the desired trajectory in advance (*182*, *228*). In both cases, the user can be hands-off.

For magnetically actuated externally steerable needles, eyes-on/hands-off and higher degrees of AI guidance have also been demonstrated. Closed-loop control has been demonstrated using feedback from camera images (*112*) and fluoroscopic images (*111*), and MRI imaging has been used to actuate needle insertion leveraging the MRI bore field itself (although in this case for a nonsteerable, straight needle) (*42*).

OPEN CHALLENGES

Translating AI-guided medical needle deployment robots from research to clinical practice is essential for real-world impact. Although many technical challenges remain, we focus here on a few critical barriers to clinical adoption, including safety, regulation, intuitive and capable physician-AI interfaces, and clinical workflow integration.

Safety and regulatory considerations

One way for AI guidance methods to address safety concerns and improve regulatory feasibility is to provide formal theoretical guarantees. Formal guarantees have been integral to verifying safety in computational systems in other application areas where the hands-off degrees of AI guidance have been successfully commercially deployed, for example, aviation autopilot systems and automotive components such as adaptive cruise control. Currently used guarantees for robots include stability guarantees in control algorithms and real-time process scheduling guarantees. However, such guarantees, although valuable, address only low-level behavior. As AI guidance methods take on higher-level responsibilities in medical needle deployment, new types of guarantees may be needed: ones that ensure that actions achieve clinical objectives safely and accurately. The challenge becomes how to formally guarantee semantic medical objectives, not just satisfy engineering constraints.

In robot motion planning, theoretical guarantees have been pursued for decades. However, because of the PSPACE-hard nature of motion planning (*229*), exact solutions in finite time are often infeasible. Instead, the field has relied on probabilistic completeness and asymptotic optimality (*230*): guarantees in the limit of computation, e.g., as computation time or power approaches infinity. Unfortunately, in medicine, the infinite limit of computation is not an ideal place to find our guarantees if guarantees are required. Recent work on motion planning for medical steerable needles has proposed algorithms that are both complete and optimal in finite time for specific designs (*176*), which is important progress in this direction.

Control methods underpinning performing motion also frequently offer critical guarantees, such as stability (*231*) and safe state set reachability (*232*). These guarantees certainly remain relevant but may be insufficient as AI guidance takes a larger role in motion execution. For instance, when full instrument state is not directly sensed, and AI guidance fills the gap, the assumptions enabling classical control guarantees may no longer hold.

Formal verification techniques, such as those based on hybrid automata, have been applied to medical robots (*233–235*). These approaches may guarantee the safety of certain AI guidance components, but applying them to the breadth of learning-based systems remains a major (and active) research challenge.

Further, current regulatory frameworks may not align with the guarantees AI systems can realistically offer. High-performing AI models are often opaque, making formal validation difficult. Efforts such as the IDEAL framework (*236*) are exploring how to adapt existing medical regulatory standards to AI-based systems, but much work remains.

Interest in regulatory and ethical considerations in this area is rapidly growing (*237*). For example, the European Union AI Act mandates human oversight for high-risk systems (*238*), emphasizing the potential importance of transparency and explainability. Explainable AI (XAI) methods (*239*) may support oversight by making AI guidance predictions interpretable. Applied to medical needle deployment, XAI may help human supervisors understand not just what the AI guidance is doing, but why. Effective supervisory methods for people who are not AI experts (but are clinical domain experts) are emerging and could potentially be integrated into clinical workflows (*240*).

Physician interfaces and clinical workflow

To be adopted in clinical settings, AI guidance for medical needle deployment robots must integrate into clinical workflows, contribute to overarching clinical objectives, and be usable by physicians. Designing effective physician interfaces for intermediate guidance modes (eyes-on/hands-on and eyes-on/hands-off; see Fig. 1) is an important challenge. Nonlinear needle paths are especially difficult to control manually (*209*, *241*), making intuitive interfaces essential. The fields of human-computer interaction (HCI) and human-robot interaction (HRI) offer valuable insights into designing such systems (*242*, *243*). Creating effective AI guidance methods for needle deployment robots will benefit from the science behind how humans and machines interact.

As AI guidance methods are tasked with higher levels of reasoning, the right way to construct these interfaces becomes less obvious. The HRI/HCI subfield of human-AI teaming is becoming increasingly relevant (*244*, *245*). A key question is how clinicians should communicate with AI systems, particularly when the AI system is involved in procedural or semantic decision-making. Foundation models such as large language models (LLMs) and vision language models (VLMs) may offer natural language interfaces for medical needle systems. LLMs tailored specifically to surgery are beginning to emerge (*246*), potentially enabling more intuitive interactions.

The physician interface is just one part of the clinical workflow. AI guidance will need to integrate seamlessly with other components, for example, real-time imaging and medical records databases, and use information from these components to learn context and patient-specific information.

Although we have highlighted a number of key areas of critical open challenges, many others remain. Bringing AI guidance of medical needle deployment robots to clinics and operating rooms, and the improved capabilities and access it will afford, will require collaborative efforts among engineers, computer scientists, and clinicians.

CONCLUSIONS

Safely and accurately navigating needles percutaneously or endoscopically to sites deep within the body is essential for many medical procedures. In this Review, we covered a wide range of applications, including biopsies, localized drug deliveries, enabling vascular access, and tumor ablations. The advent of image guidance decades ago gave physicians information about a patient's anatomy. We are now entering the era of AI guidance, where AI can automatically analyze images, identify targets and obstacles, compute safe trajectories, and autonomously navigate instruments to sites with unprecedented accuracy and precision. We surveyed recent advances in the building blocks of AI guidance for medical needles and endoscopes: perceiving anatomy, planning motions, perceiving instrument state, and performing motions. We also categorized and reviewed current needle types and robots that enable reaching sites for various applications, often with the need for obstacle avoidance. We also highlighted a number of open challenges related to safety, regulatory considerations, physician interfaces, and clinical workflow. With further advances, AI guidance for needle-based procedures has the potential to enable higher levels of automation and enhance patient care via improved accuracy and safety.

REFERENCES AND NOTES

1. C. M. McMurtry, R. P. Riddell, A. Taddio, N. Racine, G. J. G. Asmundson, M. Noel, C. T. Chambers, V. Shah, HELPinKids&Adults Team, Far from "just a poke": Common painful needle procedures and the development of needle fear. *Clin. J. Pain* **31**, S3–S11 (2015).
2. M. Silverstein, Where's the outrage? *J. Am. Coll. Surg.* **208**, 78–79 (2009).
3. S. Loeb, H. B. Carter, S. I. Berndt, W. Ricker, E. M. Schaeffer, Complications after prostate biopsy: Data from SEER-Medicare. *J. Urol.* **186**, 1830–1834 (2011).
4. J. Psaila, T. F. Parsons, S. A. Hahn, L. Fichera, Prospective study evaluating whether standard peripheral intravenous catheters can be used for blood collection throughout hospital stay. *J. Infus. Nurs.* **46**, 43–47 (2023).
5. D. G. Petereit, S. J. Frank, A. N. Viswanathan, B. Erickson, P. Eifel, P. L. Nguyen, D. E. Wazer, Brachytherapy: Where has it gone? *J. Clin. Oncol.* **33**, 980–982 (2015).
6. J.-p. Wu, J. Yu, J. B. Fowlkes, P. Liang, C. P. Nolsøe, US-guided ablation of tumors–where is it used and how did we get there. *Med-X* **1**, 5 (2023).
7. Cleveland Clinic, "Breast biopsy"; https://my.clevelandclinic.org/health/diagnostics/24204-breast-biopsy-overview.
8. M. Yip, S. Salcudean, K. Goldberg, K. Althoefer, A. Menciassi, J. D. Opfermann, A. Krieger, K. Swaminathan, C. J. Walsh, H. Huang, I.-C. Lee, Artificial intelligence meets medical robotics. *Science* **381**, 141–146 (2023).
9. D. Wu, R. Zhang, A. Pore, D. Dall'Alba, X. T. Ha, Z. Li, Y. Zhang, F. Herrera, M. Ourak, W. Kowalczyk, E. De Momi, A. Casals, J. Dankelman, J. Kober, A. Menciassi, P. Fiorini, E. Vander Poorten, A review on machine learning in flexible surgical and interventional robots: Where we are and where we are going. *Biomed. Signal Process. Control* **93**, 106179 (2024).
10. R. Galloway, T. Peters, *Overview and History of Image-Guided Interventions* (Springer, 2008).
11. Y. S. Kwoh, J. Hou, E. A. Jonckheere, S. Hayati, A robot with improved absolute positioning accuracy for CT guided stereotactic brain surgery. *IEEE Trans. Biomed. Eng.* **35**, 153–160 (1988).
12. S. Russell, P. Norvig, *Artificial Intelligence: A Modern Approach* (Pearson, ed. 4, 2020).
13. SAE International, "Taxonomy and definitions for terms related to driving automation systems for on-road motor vehicles" (30 April 2021); https://sae.org/standards/content/j3016_202104/.
14. G.-Z. Yang, J. Cambias, K. Cleary, E. Daimler, J. Drake, P. E. Dupont, N. Hata, P. Kazanzides, S. Martel, R. V. Patel, V. J. Santos, R. H. Taylor, Medical robotics—Regulatory, ethical, and legal considerations for increasing levels of autonomy. *Sci. Robot.* **2**, eaam8638 (2017).
15. A. Attanasio, B. Scaglioni, E. De Momi, P. Fiorini, P. Valdastri, Autonomy in surgical robotics. *Annu. Rev. Control Robot. Auton. Syst.* **4**, 651–679 (2021).
16. A. Lee, T. S. Baker, J. B. Bederson, B. I. Rapoport, Levels of autonomy in FDA-cleared surgical robots: A systematic review. *NPJ Digit. Med.* **7**, 103 (2024).
17. J. M. Leipheimer, M. L. Balter, A. I. Chen, E. J. Pantin, A. E. Davidovich, K. S. Labazzo, M. L. Yarmush, First-in-human evaluation of a hand-held automated venipuncture device for rapid venous blood draws. *Technology* **7**, 98–107 (2019).
18. J. G. R. Bomers, D. G. H. Bosboom, G. H. Tigelaar, J. Sabisch, J. J. Fütterer, D. Yakar, Feasibility of a 2nd generation MR-compatible manipulator for transrectal prostate biopsy guidance. *Eur. Radiol.* **27**, 1776–1782 (2017).
19. M. C. Bernardes, P. Moreira, D. Lezcano, L. Foley, K. Tuncali, C. Tempany, J. S. Kim, N. Hata, I. Iordachita, J. Tokuda, In vivo feasibility study: Evaluating autonomous data-driven robotic needle trajectory correction in MRI-guided transperineal procedures. *IEEE Robot. Autom. Lett.* **9**, 8975–8982 (2024).
20. A. Kuntz, M. Emerson, T. E. Ertop, I. Fried, M. Fu, J. Hoelscher, M. Rox, J. Akulian, E. A. Gillaspie, Y. Z. Lee, F. Maldonado, R. J. Webster III, R. Alterovitz, Autonomous medical needle steering in vivo. *Sci. Robot.* **8**, eadf761 (2023).
21. Mobileye, "Autonomous driving levels: Hands off, eyes off-a new taxonomy," 22 May 2023; https://mobileye.com/blog/hands-off-eyes-off-taxonomy-for-automated-driving/.
22. A. Shashua, S. Shalev-Shwartz, "Defining a new taxonomy for consumer autonomous vehicles," Mobileye, 6 February 2023; https://mobileye.com/opinion/defining-a-new-taxonomy-for-consumer-autonomous-vehicles/.
23. E. Franco, D. Brujic, M. Rea, W. M. Gedroyc, M. Ristic, Needle-guiding robot for laser ablation of liver tumors under MRI guidance. *IEEE ASME Trans. Mechatron.* **21**, 931–944 (2016).
24. M. G. Schouten, J. G. R. Bomers, D. Yakar, H. Huisman, E. Rothgang, D. Bosboom, T. W. J. Scheenen, S. Misra, J. J. Fütterer, Evaluation of a robotic technique for transrectal MRI-guided prostate biopsies. *Eur. Radiol.* **22**, 476–483 (2012).
25. D. Stoianovici, C. Kim, D. Petrisor, C. Jun, S. Lim, M. W. Ball, A. Ross, K. J. Macura, M. E. Allaf, MR safe robot, FDA clearance, safety and feasibility of prostate biopsy clinical trial. *IEEE ASME Trans. Mechatron.* **22**, 115–126 (2017).
26. B. Maris, C. Tenga, R. Vicario, L. Palladino, N. Murr, M. De Piccoli, A. Calanca, S. Puliatti, S. Micali, A. Tafuri, P. Fiorini, Toward autonomous robotic prostate biopsy: A pilot study. *Int. J. Comput. Assist. Radiol. Surg.* **16**, 1393–1401 (2021).
27. M. K. Welleweerd, F. J. Siepel, V. Groenhuis, J. Veltman, S. Stramigioli, Design of an end-effector for robot-assisted ultrasound-guided breast biopsies. *Int. J. Comput. Assist. Radiol. Surg.* **15**, 681–690 (2020).
28. Z. Cheng, B. Many, K. B. Jørgensen, S. An, M. L. Jensen, R. Thulstrup, H. Frost, T. R. Savarimuthu, O. Huldt, "Portable robot for needle insertion assistance to femoral artery" in *2024 IEEE/RSJ International Conference on Intelligent Robots and Systems (IROS)* (IEEE, 2024), pp. 2407–2413.
29. Interventional Systems, "Micromate"; https://interventional-systems.com.
30. Zimmer Biomet, "ROSA One Brain"; https://zimmerbiomet.com/en/products-and-solutions/zb-edge/robotics/rosa-brain.html.
31. Renishaw, "Neuromate robotic system for stereotactic neurosurgery"; https://renishaw.com/en/neuromate-robotic-system-for-stereotactic-neurosurgery--10712.
32. Biobot Surgical, "iSR'OBOT Mona Lisa"; https://biobotsurgical.com/technology/.
33. Zhongyi Medical, "AmaKris SR1-A"; https://en.aimsrobots.com/product/7.html.
34. H. Ranjan, M. Van Hilten, V. Groenhuis, J. Verde, A. Garcia, S. Perretta, J. Veltman, F. J. Siepel, S. Stramigioli, "Sunram 7: An MR safe robotic system for breast biopsy" in *2023 IEEE/RSJ International Conference on Intelligent Robots and Systems (IROS)* (IEEE, 2023), pp. 10281–10288.
35. D. Stoianovici, J. A. Cadeddu, R. D. Demaree, S. A. Basile, R. H. Taylor, L. L. Whitcomb, W. N. Sharpe Jr., L. R. Kavoussi, "An efficient needle injection technique and radiological guidance method for percutaneous procedures" in *International Conference on Computer Vision, Virtual Reality, and Robotics in Medicine* (Springer, 1997), pp. 295–298.
36. D. Stoianovici, K. Cleary, A. Patriciu, D. Mazilu, A. Stanimir, N. Craciunoiu, V. Watson, L. Kavoussi, AcuBot: A robot for radiological interventions. *IEEE Trans. Robot. Autom.* **19**, 927–930 (2003).
37. C. J. Walsh, N. C. Hanumara, A. H. Slocum, J.-A. Shepard, R. Gupta, A patient-mounted, telerobotic tool for CT-guided percutaneous interventions. *J. Med. Devices* **2**, 011007 (2008).
38. O. Piccin, L. Barbé, B. Bayle, M. de Mathelin, A. Gangi, A force feedback teleoperated needle insertion device for percutaneous procedures. *Int. J. Robot Res.* **28**, 1154–1168 (2009).
39. T. Nakano, N. Sugita, T. Ueta, Y. Tamaki, M. Mitsuishi, A parallel robot to assist vitreoretinal surgery. *Int. J. Comput. Assist. Radiol. Surg.* **4**, 517–526 (2009).
40. P. Vartholomeos, L. Qin, P. E. Dupont, "MRI-powered actuators for robotic interventions" in *IEEE/RSJ International Conference on Intelligent Robots and Systems (IROS)* (IEEE, 2011), pp. 4508–4515.
41. C. Bergeles, L. Qin, P. Vartholomeos, P. E. Dupont, "Tracking and position control of an MRI-powered needle-insertion robot" in *2012 Annual International Conference of the IEEE Engineering in Medicine and Biology Society (EMBS)* (IEEE, 2012), pp. 928–931.
42. P. Vartholomeos, C. Bergeles, L. Qin, P. E. Dupont, An MRI-powered and controlled actuator technology for tetherless robotic interventions. *Int. J. Robot Res.* **32**, 1536–1552 (2013).

43. E. Rahimy, J. Wilson, T. C. Tsao, S. Schwartz, J.-P. Hubschman, Robot-assisted intraocular surgery: Development of the IRISS and feasibility studies in an animal model. *Eye* **27**, 972–978 (2013).
44. G. Li, H. Su, W. Shang, J. Tokuda, N. Hata, C. M. Tempany, G. S. Fischer, "A fully actuated robotic assistant for MRI-guided prostate biopsy and brachytherapy" in *Medical Imaging 2013: Image-Guided Procedures, Robotic Interventions, and Modeling* (SPIE, 2013), vol. 8671, pp. 311–318.
45. M. L. Balter, A. I. Chen, T. J. Maguire, M. L. Yarmush, The system design and evaluation of a 7-DOF image-guided venipuncture robot. *IEEE Trans. Robot.* **31**, 1044–1053 (2015).
46. N. Hungr, I. Bricault, P. Cinquin, C. Fouard, Design and validation of a CT- and MRI-guided robot for percutaneous needle procedures. *IEEE Trans. Robot.* **32**, 973–987 (2016).
47. M. Nambi, P. S. Bernstein, J. J. Abbott, A compact telemanipulated retinal-surgery system that uses commercially available instruments with a quick-change adapter. *J. Med. Robot. Res.* **1**, 1630001 (2016).
48. V. Groenhuis, S. Stramigioli, Laser-cutting pneumatics. *IEEE ASME Trans. Mechatron.* **21**, 1604–1611 (2016).
49. M. Ye, W. Li, D. T. M. Chan, P. W. Y. Chiu, Z. Li, A semi-autonomous stereotactic brain biopsy robot with enhanced safety. *IEEE Robot. Autom. Lett.* **5**, 1405–1412 (2020).
50. L. Brattain, T. T. Pierce, L. A. Gjesteby, M. R. Johnson, N. D. DeLosa, J. S. Werblin, J. F. Gupta, A. Ozturk, X. Wang, Q. Li, B. A. Telfer, A. E. Samir, AI-Enabled, ultrasound-guided handheld robotic device for femoral vascular access. *Biosensors* **11**, 522 (2021).
51. M. J. Musa, K. Sharma, K. Cleary, Y. Chen, Respiratory compensated robot for liver cancer treatment: Design, fabrication, and benchtop characterization. *IEEE ASME Trans. Mechatron.* **27**, 268–279 (2022).
52. M. Zhou, X. Guo, M. Grimm, E. Lochner, Z. Jiang, A. Eslami, J. Ye, N. Navab, A. Knoll, M. A. Nasseri, Needle detection and localisation for robot-assisted subretinal injection using deep learning. *CAAI Trans. Intell. Technol.* 10.1049/cit2.12242 (2023).
53. M. Koskinopoulou, A. Acemoglu, V. Penza, L. S. Mattos, "Dual robot collaborative system for autonomous venous access based on ultrasound and bioimpedance sensing technology" in *2023 IEEE International Conference on Robotics and Automation (ICRA)* (IEEE, 2023), pp. 4648–4653.
54. Z. Yang, S. Wen, Q. Qi, Z. Lv, A. Ji, A trocar puncture robot for assisting venipuncture blood collection. *Robotica* **42**, 1597–1613 (2024).
55. Z. Liang, C. Lu, H. Yang, R. Hashem, M. E. Abdelaziz, L. Lindenroth, S. Bandula, D. Stoyanov, A. Stilli, "An MR safe double-arch needle insertion robot with scissor-folding mechanism for abdominal percutaneous interventions" in *2024 IEEE/RSJ International Conference on Intelligent Robots and Systems (IROS)* (IEEE, 2024), pp. 11010–11017.
56. G. S. Fischer, I. Iordachita, C. Csoma, J. Tokuda, S. P. DiMaio, C. M. Tempany, N. Hata, G. Fichtinger, MRI-compatible pneumatic robot for transperineal prostate needle placement. *IEEE ASME Trans. Mechatron.* **13**, 295–305 (2008).
57. D. Stoianovici, C. Kim, G. Srimathveeravalli, P. Sebrecht, D. Petrisor, J. Coleman, S. B. Solomon, H. Hricak, MRI-safe robot for endorectal prostate biopsy. *IEEE ASME Trans. Mechatron.* **19**, 1289–1299 (2013).
58. N. Zevallos, E. Harber, K. Patel, Y. Gu, K. Sladick, F. Guyette, L. Weiss, M. R. Pinsky, H. Gomez, J. Galeotti, H. Choset, "Toward robotically automated femoral vascular access" in *2021 International Symposium on Medical Robotics (ISMR)* (IEEE, 2021), pp. 1–7.
59. J. Leipheimer, M. Balter, A. Chen, M. Yarmush, Design and evaluation of a handheld robotic device for peripheral catheterization. *J. Med. Device.* **16**, 021015 (2022).
60. P. Carvalho, A. Kesari, S. Weaver, P. Flaherty, G. S. Fischer, "Robotic assistive device for phlebotomy" in *International Design Engineering Technical Conferences and Computers and Information in Engineering Conference (IDETC-CIE)* (ASME 2015), vol. 3, p. V003T14A012.
61. B. Guiu, T. De Baère, G. Noel, M. Ronot, Feasibility, safety and accuracy of a CT-guided robotic assistance for percutaneous needle placement in a swine liver model. *Sci. Rep.* **11**, 5218 (2021).
62. S. Ferrari, E. Tagliabue, B. M. Maris, P. Fiorini, Autonomous robotic system for breast biopsy with deformation compensation. *IEEE Robot. Autom. Lett.* **8**, 1215–1222 (2023).
63. T. L. Edwards, K. Xue, H. C. M. Meenink, M. J. Beelen, G. J. L. Naus, M. P. Simunovic, M. Latasiewicz, A. D. Farmery, M. D. De Smet, R. E. MacLaren, First-in-human study of the safety and viability of intraocular robotic surgery. *Nat. Biomed. Eng.* **2**, 649–656 (2018).
64. M. Zimmermann, R. Krishnan, A. Raabe, V. Seifert, Robot-assisted navigated endoscopic ventriculostomy: Implementation of a new technology and first clinical results. *Acta Neurochir.* **146**, 697–704 (2004).
65. F. Turgut, G. M. Somfai, F. M. Heussen, A. Eberle, M. D. de Smet, M. D. Becker, Robotassisted epiretinal membrane peeling: a prospective assessment of pre-and intra-operative times and of surgeons' subjective perceptions. *J. Clin. Med.* **12**, 2768 (2023).
66. J. A. Cadeddu, D. Stoianovici, R. N. Chen, R. G. Moore, L. R. Kavoussi, Stereotactic mechanical percutaneous renal access. *J. Endourol.* **12**, 121–125 (1998).
67. Zeiss, "Preceyes Surgical System"; https://preceyes.nl/.
68. N. J. Cowan, K. Goldberg, G. S. Chirikjian, G. Fichtinger, R. Alterovitz, K. B. Reed, V. Kallem, W. Park, S. Misra, A. M. Okamura, "Robotic needle steering: Design, modeling, planning, and image guidance" in *Surgical Robotics: Systems Applications and Visions*, J. Rosen, B. Hannaford, R. M. Satava, Eds. (Springer, 2011), pp. 557–582.
69. J. Burgner-Kahrs, D. C. Rucker, H. Choset, Continuum robots for medical applications: A survey. *IEEE Trans. Robot.* **31**, 1261–1280 (2015).
70. F. J. Siepel, B. Maris, M. K. Welleweerd, V. Groenhuis, P. Fiorini, S. Stramigioli, Needle and biopsy robots: A review. *Curr. Robot. Rep.* **2**, 73–84 (2021).
71. P. E. Dupont, N. Simaan, H. Choset, C. Rucker, Continuum robots for medical interventions. *Proc. IEEE* **110**, 847–870 (2022).
72. N. J. van de Berg, D. J. van Gerwen, J. Dankelman, J. J. van den Dobbelsteen, Design choices in needle steering—A review. *IEEE ASME Trans. Mechatron.* **20**, 2172–2183 (2014).
73. M. Babaiasl, F. Yang, J. P. Swensen, Robotic needle steering: State-of-the-art and research challenges. *Intell. Serv. Robot.* **15**, 679–711 (2022).
74. M. Lu, Y. Zhang, C. M. Lim, H. Ren, Flexible needle steering with tethered and untethered actuation: Current states, targeting errors, challenges and opportunities. *Ann. Biomed. Eng.* **51**, 905–924 (2023).
75. S. Yu, Y. Lim, S. Kim, S. C. Ryu, Design and mechanics of active needles: A review. *IEEE Trans. Med. Robot. Bionics* **7**, 189–199 (2025).
76. R. J. Webster III, J. S. Kim, N. J. Cowan, G. S. Chirikjian, A. M. Okamura, Nonholonomic modeling of needle steering. *Int. J. Robot Res.* **25**, 509–525 (2006).
77. R. Alterovitz, K. Goldberg, A. M. Okamura, "Planning for steerable bevel-tip needle insertion through 2D soft tissue with obstacles" in *Proceedings of the 2005 IEEE International Conference on Robotics and Automation (ICRA)* (IEEE, 2005), pp. 1652–1657.
78. R. J. Webster, III, N. J. Cowan, G. Chirikjian, A. M. Okamura, "Nonholonomic modeling of needle steering" in *Experimental Robotics IX*, M. H. Ang, O. Khatib, Eds., vol. 21 of *Springer Tracts in Advanced Robotics* (Springer-Verlag, 2006), pp. 35–44.
79. W. Park, J. S. Kim, Y. Zhou, N. J. Cowan, A. M. Okamura, G. S. Chirikjian, "Diffusion-based motion planning for a nonholonomic flexible needle model" in *Proceedings of the 2005 IEEE International Conference on Robotics and Automation (ICRA)* (IEEE, 2005), pp. 4611–4616.
80. D. S. Minhas, J. A. Engh, M. M. Fenske, C. N. Riviere, "Modeling of needle steering via duty-cycled spinning" in *2007 29th Annual International Conference of the IEEE Engineering in Medicine and Biology Society (EMBS)* (IEEE, 2007), pp. 2756–2759.
81. T. R. Wedlick, A. M. Okamura, "Characterization of pre-curved needles for steering in tissue" in *2009 Annual International Conference of the IEEE Engineering in Medicine and Biology Society (EMBS)* (IEEE, 2009), pp. 1200–1203.
82. P. J. Swaney, J. Burgner, H. B. Gilbert, R. J. Webster III, A flexure-based steerable needle: High curvature with reduced tissue damage. *IEEE Trans. Biomed. Eng.* **60**, 906–909 (2013).
83. M. Rox, M. Emerson, T. E. Ertop, I. Fried, M. Fu, J. Hoelscher, A. Kuntz, J. Granna, J. E. Mitchell, M. Lester, F. Maldonado, E. A. Gillaspie, J. A. Akulian, R. Alterovitz, R. J. Webster III, Decoupling steerability from diameter: Helical dovetail laser patterning for steerable needles. *IEEE Access* **8**, 181411–181419 (2020).
84. S. Okazawa, R. Ebrahimi, J. Chuang, S. E. Salcudean, R. Rohling, Hand-held steerable needle device. *IEEE ASME Trans. Mechatron.* **10**, 285–296 (2005).
85. R. J. Roesthuis, N. J. van de Berg, J. J. van den Dobbelsteen, S. Misra, "Modeling and steering of a novel actuated-tip needle through a soft-tissue simulant using fiber Bragg grating sensors" in *International Conference on Robotics and Automation (ICRA)* (IEEE, 2015), pp. 2283–2289.
86. T. K. Adebar, J. D. Greer, P. F. Laeseke, G. L. Hwang, A. M. Okamura, Methods for improving the curvature of steerable needles in biological tissue. *IEEE Trans. on Biomed. Eng.* **63**, 1167–1177 (2016).
87. A. Yamada, S. Naka, N. Nitta, S. Morikawa, T. Tani, A loop-shaped flexible mechanism for robotic needle steering. *IEEE Robot. Autom. Lett.* **3**, 648–655 (2018).
88. M. de Vries, J. Sikorski, S. Misra, J. J. van den Dobbelsteen, Axially rigid steerable needle with compliant active tip control. *PLOS ONE* **16**, e0261089 (2021).
89. E. Ayvali, J. P. Desai, "Towards a discretely actuated steerable cannula" in *2012 IEEE International Conference on Robotics and Automation (ICRA)* (IEEE, 2012), pp. 1614–1619.
90. S. C. Ryu, Z. F. Quek, J.-S. Koh, P. Renaud, R. J. Black, B. Moslehi, B. L. Daniel, K.-J. Cho, M. R. Cutkosky, Design of an optically controlled MR-compatible active needle. *IEEE Trans. Robot.* **31**, 1–11 (2015).
91. B. Konh, D. Sasaki, T. K. Podder, H. Ashrafiuon, 3D manipulation of an active steerable needle via actuation of multiple SMA wires. *Robotica* **38**, 410–426 (2020).
92. L. Frasson, S. Y. Ko, A. Turner, T. Parittotokkaporn, J. F. Vincent, F. Rodriguez y Baena, STING: A soft-tissue intervention and neurosurgical guide to access deep brain lesions through curved trajectories. *Proc. Inst. Mech. Eng. H* **224**, 775–788 (2010).
93. A. Aktas, A. A. Demircali, R. Secoli, B. Temelkuran, F. Rodriguez y Baena, Towards a procedure-optimised steerable catheter for deep-seated neurosurgery. *Biomedicines* **11**, 2008 (2023).
94. M. Babaiasl, F. Yang, S. Boccelli, J. P. Swensen, "Fracture-directed waterjet needle steering: Design, modeling, and path planning" in *Proceedings of IEEE International Conference on Biomedical Robotics and Biomechatronics (BioRob)* (IEEE, 2020), pp. 1166–1173.
95. F. Yang, M. Babaiasl, J. P. Swensen, Fracture-directed steerable needles. *J. Med. Robot. Res.* **4**, 1842002 (2019).

96. R. Secoli, E. Matheson, M. Pinzi, S. Galvan, A. Donder, T. Watts, M. Riva, D. D. Zani, L. Bello, F. Rodriguez y Baena, Modular robotic platform for precision neurosurgery with a bio-inspired needle: System overview and first in-vivo deployment. *PLOS ONE* **17**, e0275686 (2022).
97. S. P. DiMaio, S. E. Salcudean, Needle steering and motion planning in soft tissues. *IEEE Trans. Biomed. Eng.* **52**, 965–974 (2005).
98. D. Glozman, M. Shoham, Image-guided robotic flexible needle steering. *IEEE Trans. Robot.* **23**, 459–467 (2007).
99. Xact Robotics, "Ace robotic system"; https://xactrobotics.com/ace-robotic-system/.
100. J. Granna, E. B. Pitt, M. E. McKay, T. J. Ball, J. S. Neimat, D. J. Englot, R. P. Naftel, E. J. Barth, R. J. Webster III, Targeting epilepsy through the foremen ovale: How many helical needles are needed? *Ann. Biomed. Eng.* **50**, 499–506 (2022).
101. P. Sears, P. Dupont, "A steerable needle technology using curved concentric tubes" in *2006 IEEE International Conference on Intelligent Robots and Systems (IROS)* (IEEE, 2006), pp. 2850–2856.
102. R. J. Webster, A. M. Okamura, N. J. Cowan, "Toward active cannulas: Miniature snakelike surgical robots" in *2006 IEEE/RSJ International Conference on Intelligent Robots and Systems (IROS)* (IEEE, 2006), pp. 2857–2863.
103. P. E. Dupont, J. Lock, B. Itkowitz, E. Butler, Design and control of concentric-tube robots. *IEEE Trans. Robot.* **26**, 209–225 (2010).
104. D. C. Rucker, R. J. Webster III, Statics and dynamics of continuum robots with general tendon routing and external loading. *IEEE Trans. Robot.* **27**, 1033–1044 (2011).
105. C. Bedell, J. Lock, A. Gosline, P. E. Dupont, "Design optimization of concentric tube robots based on task and anatomical constraints" in *IEEE International Conference on Robotics and Automation (ICRA)* (IEEE, 2011), pp. 398–403.
106. H. B. Gilbert, J. Neimat, R. J. Webster III, Concentric tube robots as steerable needles: Achieving follow-the-leader deployment. *IEEE Trans. Robot.* **31**, 246–258 (2015).
107. C. Girerd, K. Rabenorosoa, P. Rougeot, P. Renaud, "Towards optical biopsy of olfactory cells using concentric tube robots with follow-the-leader deployment" in *2017 IEEE/RSJ International Conference on Intelligent Robots and Systems (IROS)* (IEEE, 2017), pp. 5661–5887.
108. H. Choset, W. Henning, A follow-the-leader approach to serpentine robot motion planning. *J. Aerosp. Eng.* **12**, 65–73 (1999).
109. B. J. Nelson, S. Gervasoni, P. W. Y. Chiu, L. Zhang, A. Zemmar, Magnetically actuated medical robots: An in vivo perspective. *Proc. IEEE* **110**, 1028–1037 (2022).
110. M. Ilami, R. J. Ahmed, A. Petras, B. Beigzadeh, H. Marvi, Magnetic needle steering in soft phantom tissue. *Sci. Rep.* **10**, 2500 (2020).
111. A. Hong, A. J. Petruska, A. Zemmar, B. J. Nelson, Magnetic control of a flexible needle in neurosurgery. *IEEE Trans. Biomed. Eng.* **68**, 616–627 (2021).
112. A. J. Petruska, F. Ruetz, A. Hong, L. Regli, O. Sürücü, A. Zemmar, B. J. Nelson, "Magnetic needle guidance for neurosurgery: Initial design and proof of concept" in *2015 IEEE International Conference on Robotics and Automation (ICRA)* (IEEE, 2016), pp. 4392–4397.
113. A. J. Sperry, T. J. Schwehr, E. K. Pinegar, O. B. Richards, J. D. Rolston, M. D. Alexander, B. Coats, J. J. Abbott, A. Kuntz, Screw-tip soft magnetically steerable needles. *IEEE Trans. Med. Robot. Bionics* **6**, 4–17 (2024).
114. P. Kheradmand, B. Moradkhani, H. Jella, K. Sowards, S. R. Silva, Y. Chitalia, Towards a tendon-assisted magnetically steered (TAMS) robotic stylet for brachytherapy. *IEEE Robot. Autom. Lett.* **9**, 6464–6471 (2024).
115. M. Torabi, K. Hauser, R. Alterovitz, V. Duindam, K. Goldberg, Guiding medical needles using single-point tissue manipulation, in *2009 IEEE International Conference on Robotics and Automation (ICRA)* (IEEE, 2009), pp. 2705–2710.
116. Y. Zou, B. Guan, J. Zhao, S. Wang, X. Sun, J. Li, Robotic-assisted automatic orientation and insertion for bronchoscopy based on image guidance. *IEEE Trans. Med. Robot. Bionics* **4**, 588–598 (2022).
117. J. Zhang, L. Liu, P. Xiang, Q. Fang, X. Nie, H. Ma, J. Hu, R. Xiong, Y. Wang, H. Lu, AI co-pilot bronchoscope robot. *Nat. Commun.* **15**, 241 (2024).
118. Y. Chen, J. Liang, I. W. Hunter, "Modular continuum robotic endoscope design and path planning" in *2014 IEEE International Conference on Robotics and Automation (ICRA)* (IEEE, 2014), pp. 5393–5400.
119. Y. Gao, K. Takagi, T. Kato, N. Shono, N. Hata, Continuum robot with follow-the-leader motion for endoscopic third ventriculostomy and tumor biopsy. *IEEE Trans. Biomed. Eng.* **67**, 379–390 (2020).
120. J. W. Martin, L. Barducci, B. Scaglioni, J. C. Norton, C. Winters, V. Subramanian, A. Arezzo, K. L. Obstein, P. Valdastri, Robotic autonomy for magnetic endoscope biopsy. *IEEE Trans. Med. Robot. Bionics* **4**, 599–607 (2022).
121. M. Verra, A. Firrincieli, M. Chiurazzi, A. Mariani, G. Lo Secco, E. Forcignanò, A. Koulaouzidis, A. Menciassi, P. Dario, G. Ciuti, A. Arezzo, Robotic-assisted colonoscopy platform with a magnetically-actuated soft-tethered capsule. *Cancers* **12**, 2485 (2020).
122. P. Valdastri, G. Ciuti, A. Verbeni, A. Menciassi, P. Dario, A. Arezzo, M. Morino, Magnetic air capsule robotic system: Proof of concept of a novel approach for painless colonoscopy. *Surg. Endosc.* **26**, 1238–s1246 (2012).
123. Y. Li, C. Guo, W. Xin, T. Pan, W. Li, P. W. Y. Chiu, Z. Li, Design and preliminary evaluation of an electromagnetically actuated soft-tethered colonoscope. *IEEE Trans. Med. Robot. Bionics* **3**, 402–413 (2021).
124. A. Kuntz, L. G. Torres, R. H. Feins, R. J. Webster III, R. Alterovitz, "Motion planning for a three-stage multilumen transoral lung access system" in 2015 *IEEE/RSJ International Conference on Intelligent Robots and Systems (IROS)* (IEEE, 2015), pp. 3255–3261.
125. S. Amack, M. Rox, J. Mitchell, T. E. Ertop, M. Emerson, A. Kuntz, F. Maldonado, J. Akulian, J. Gafford, R. Alterovitz, R. J. Webster III, "Design and control of a compact modular robot for transbronchial lung biopsy" in *Medical Imaging 2019: Image-Guided Procedures, Robotic Interventions, and Modeling* (International Society for Optics and Photonics, 2019), p. 109510I.
126. K. L. Obstein, C. A. Landewee, J. Norton, J. Martin, S. Caló, J. W. Kow, B. Scaglioni, P. Valdastri, The magnetic flexible endoscope: Phase 1 first-in-human trial. *Am. J. Gastroenterol.* 10.14309/ajg.0000000000003584 (2025).
127. Johnson&Johnson MedTech, "Monarch bronchoscopy"; https://jnjmedtech.com/en-US/product-family/monarch.
128. Intuitive Surgical, "Ion"; https://intuitive.com/en-us/about-us/newsroom/press-resources.
129. S. E. Salcudean, H. Moradi, D. G. Black, N. Navab, Robot-assisted medical imaging: A review. *Proc. IEEE* **110**, 951–967 (2022).
130. T. S. Yoo, *Insight into Images: Principles and Practice for Segmentation, Registration, and Image Analysis* (AK Peters Ltd., 2004).
131. D. Schreiber, Z. Yu, T. Henderson, D. Chen, A. Norbash, M. C. Yip, CRANE: A redundant, multi-degree-of-freedom computed tomography robot for heightened needle dexterity within a medical imaging bore. *IEEE Trans. Robot.* 10.1109/TRO.2024.3364986 (2024).
132. M. Fu, A. Kuntz, R. J. Webster III, R. Alterovitz, "Safe motion planning for steerable needles using cost maps automatically extracted from pulmonary images" in *2018 IEEE/RSJ International Conference on Intelligent Robots and Systems (IROS)* (IEEE, 2018), pp. 4942–4949.
133. A. Segato, C. Di Vece, S. Zucchelli, M. Di Marzo, T. Wendler, M. F. Azampour, S. Galvan, R. Secoli, E. De Momi, Position-based dynamics simulator of brain deformations for path planning and intra-operative control in keyhole neurosurgery. *IEEE Robot. Autom. Lett.* **6**, 6061–6067 (2021).
134. D. Shen, G. Wu, H.-I. Suk, Deep learning in medical image analysis. *Annu. Rev. Biomed. Eng.* **19**, 221–248 (2017).
135. G. Litjens, T. Kooi, B. E. Bejnordi, A. A. A. Setio, F. Ciompi, M. Ghafoorian, J. A. W. M. Van Der Laak, B. Van Ginneken, C. I. Sánchez, A survey on deep learning in medical image analysis. *Med. Image Anal.* **42**, 60–88 (2017).
136. D. Stoianovici, Multi-imager compatible actuation principles in surgical robotics. *Int. J. Med. Robot.* **1**, 86–100 (2005).
137. R. Seifabadi, I. Iordachita, G. Fichtinger, "Design of a teleoperated needle steering system for MRI-guided prostate interventions" in *Proceedings of the International Conference on Biomedical Robotics and Biomechatronics (BioRob)* (IEEE, 2012), pp. 793–798.
138. J. Bloemberg, F. Trauzettel, B. Coolen, D. Dodou, P. Breedveld, Design and evaluation of an MRI-ready, self-propelled needle for prostate interventions. *PLOS ONE* **17**, e0274063 (2022).
139. D. Yakar, M. G. Schouten, D. G. H. Bosboom, J. O. Barentsz, T. W. J. Scheenen, J. J. Fütterer, Feasibility of a pneumatically actuated MR-compatible robot for transrectal prostate biopsy guidance. *Radiology* **260**, 241–247 (2011).
140. S. Lim, C. Jun, D. Chang, D. Petrisor, M. Han, D. Stoianovici, Robotic transrectal ultrasound guided prostate biopsy. *IEEE Trans. Biomed. Eng.* **66**, 2527–2537 (2019).
141. M. Abayazid, P. Moreira, N. Shahriari, S. Patil, R. Alterovitz, S. Misra, Ultrasound-guided three-dimensional needle steering in biological tissue with curved surfaces. *Med. Eng. Phys.* **37**, 145–150 (2015).
142. M. Aggravi, D. A. Estima, A. Krupa, S. Misra, C. Pacchierotti, Haptic teleoperation of flexible needles combining 3D ultrasound guidance and needle tip force feedback. *IEEE Robot. Autom. Lett.* **6**, 4859–4866 (2021).
143. F. Abhimanyu, A. L. Orekhov, A. Bal, J. Galeotti, H. Choset, "Unsupervised deformable ultrasound image registration and its application for vessel segmentation" in *2023 IEEE/RSJ International Conference on Intelligent Robots and Systems (IROS)* (IEEE, 2023), pp. 6579–6585.
144. L. Lei, B. Zhao, X. Qi, R. Mi, H. Ye, P. Zhang, Q. Wang, P.-A. Heng, Y. Hu, Robotic needle insertion with 2D ultrasound–3D CT fusion guidance. *IEEE Trans. Autom. Sci. Eng.* **21**, 6152–6164 (2024).
145. A. I. Chen, M. L. Balter, T. J. Maguire, M. L. Yarmush, Deep learning robotic guidance for autonomous vascular access. *Nat. Mach. Intell.* **2**, 104–115 (2020).
146. B. D. Killeen, C. Gao, K. J. Oguine, S. Darcy, M. Armand, R. H. Taylor, G. Osgood, M. Unberath, An autonomous X-ray image acquisition and interpretation system for assisting percutaneous pelvic fracture fixation. *Int. J. Comput. Assist. Radiol. Surg.* **18**, 1201–1208 (2023).
147. M. Visentini-Scarzanella, T. Sugiura, T. Kaneko, S. Koto, Deep monocular 3D reconstruction for assisted navigation in bronchoscopy. *Int. J. Comput. Assist. Radiol. Surg.* **12**, 1089–1099 (2017).

148. C. Wang, M. Oda, Y. Hayashi, B. Villard, T. Kitasaka, H. Takabatake, M. Mori, H. Honma, H. Natori, K. Mori, A visual SLAM-based bronchoscope tracking scheme for bronchoscopic navigation. *Int. J. Comput. Assist. Radiol. Surg.* **15**, 1619–1630 (2020).
149. P. Vagdargi, A. Uneri, S. Liu, C. K. Jones, A. Sisniega, J. Lee, P. A. Helm, W. S. Anderson, M. Luciano, G. D. Hager, J. H. Siewerdsen, "End-to-end 3D neuroendoscopic video reconstruction for robot-assisted ventriculostomy" in *Medical Imaging 2024: Image-Guided Procedures, Robotic Interventions, and Modeling* (SPIE, 2024), pp. 128–133.
150. R. Ma, R. Wang, Y. Zhang, S. Pizer, S. K. McGill, J. Rosenman, J.-M. Frahm, RNNSLAM: Reconstructing the 3D colon to visualize missing regions during a colonoscopy. *Med. Image Anal.* **72**, 102100 (2021).
151. A. Wankhede, L. Madiraju, D. Patel, K. Cleary, C. Oluigbo, R. Monfaredi, "Heuristic-based optimal path planning for neurosurgical tumor ablation" in *Medical Imaging 2019: ImageGuided Procedures, Robotic Interventions, and Modeling* (SPIE, 2019), pp. 655–663.
152. V. Groenhuis, F. J. Siepel, S. Stramigioli, "Sunram 5: A magnetic resonance-safe robotic system for breast biopsy, driven by pneumatic stepper motors" in *Handbook of Robotic and Image-Guided Surgery* (Elsevier, 2020), pp. 375–396.
153. R. Alterovitz, K. Goldberg, J. Pouliot, R. Taschereau, "Sensorless planning for medical needle insertion procedures" in *2003 IEEE/RSJ International Conference on Intelligent Robots and Systems (IROS)* (IEEE, 2005), vol. 3, pp. 3337–3343.
154. C. Villard, C. Baegert, P. Schreck, L. Soler, A. Gangi, "Optimal trajectories computation within regions of interest for hepatic RFA planning" in *International Conference on Medical Image Computing and Computer-Assisted Intervention* (Springer, 2005), pp. 49–56.
155. E. De Momi, C. Caborni, F. Cardinale, L. Castana, G. Casaceli, M. Cossu, L. Antiga, G. Ferrigno, Automatic trajectory planner for stereoelectroencephalography procedures: A retrospective study. *IEEE Trans. Biomed. Eng.* **60**, 986–993 (2013).
156. A. Seitel, M. Engel, C. M. Sommer, B. A. Radeleff, C. Essert-Villard, C. Baegert, M. Fangerau, K. H. Fritzsche, K. Yung, H.-P. Meinzer, L. Maier-Hein, Computer-assisted trajectory planning for percutaneous needle insertions. *Med. Phys.* **38**, 3246–3259 (2011).
157. F. Li, Z. Huang, L. Xu, "Path planning of 6-DOF venipuncture robot arm based on improved A-star and collision detection algorithms" in *2019 IEEE International Conference on Robotics and Biomimetics (ROBIO)* (IEEE, 2019), pp. 2971–2976.
158. R. Alterovitz, A. Lim, K. Goldberg, G. S. Chirikjian, A. M. Okamura, "Steering flexible needles under Markov motion uncertainty" in *2005 IEEE/RSJ International Conference on Intelligent Robots and Systems (IROS)* (IEEE, 2005), pp. 120–125.
159. R. Alterovitz, M. Branicky, K. Goldberg, "Constant-curvature motion planning under uncertainty with applications in image-guided medical needle steering" in *Algorithmic Foundation of Robotics VII (Proceedings of WAFR 2006)* (Springer-Verlag, 2008), vol. 47 of *Springer Tracts in Advanced Robotics*, pp. 319–334.
160. R. Alterovitz, M. Branicky, K. Goldberg, Motion planning under uncertainty for image-guided medical needle steering. *Int. J. Rob. Res.* **27**, 1361–1374 (2008).
161. W. Park, J. S. Kim, Y. Zhou, N. J. Cowan, A. M. Okamura, G. S. Chirikjian, "Diffusion-based motion planning for a nonholonomic flexible needle model" in *Proceedings of IEEE International Conference on Robotics and Automation (ICRA)* (IEEE, 2005), pp. 4611–4616.
162. V. Duindam, J. Xu, R. Alterovitz, S. Sastry, K. Goldberg, 3D motion planning algorithms for steerable needles using inverse kinematics. *Int. J. Rob. Res.* **29**, 789–800 (2010).
163. S. Bano, S. Y. Ko, F. Rodriguez y Baena, "Smooth path planning for a biologically inspired neurosurgical probe" in *Annual International Conference of the IEEE Engineering in Medicine and Biology Society (EMBS)* (IEEE, 2012), pp. 920–923.
164. A. Segato, V. Corbetta, J. Zangari, S. Perri, F. Calimeri, E. De Momi, "Optimized 3D path planner for steerable catheters with deductive reasoning" in *International Conference on Robotics and Automation (ICRA)* (IEEE, 2021), pp. 1466–1472.
165. J. Xu, V. Duindam, R. Alterovitz, K. Goldberg, "Motion planning for steerable needles in 3D environments with obstacles using rapidly-exploring random trees and backchaining" in *Proceedings of IEEE International Conference on Automation Science and Engineering (CASE)* (IEEE, 2008), pp. 41–46.
166. S. Patil, R. Alterovitz, "Interactive motion planning for steerable needles in 3D environments with obstacles" in *Proceedings of IEEE International Conference on Biomedical Robotics and Biomechatronics (BioRob)* (IEEE, 2010), pp. 893–899.
167. C. Caborni, S. Y. Ko, E. De Momi, G. Ferrigno, F. Rodriguez y Baena, "Risk-based path planning for a steerable flexible probe for neurosurgical intervention" in *Proceedings of IEEE International Conference on Biomedical Robotics and Biomechatronics (BioRob)* (IEEE, 2012), pp. 866–871.
168. Y.-J. Zhao, B. Konh, M. Honarvar, F. O. M. Joseph, T. K. Podder, P. Hutapea, A. P. Dicker, Y. Yu, 3D motion planning for robot-assisted active flexible needle based on rapidly exploring random trees. *J. Autom. Control Eng.* **3**, 360–367 (2015).
169. W. Sun, J. van den Berg, R. Alterovitz, Stochastic extended LQR for optimization-based motion planning under uncertainty. *IEEE Trans. Autom. Sci. Eng.* **13**, 437–447 (2016).
170. M. Bentley, D. C. Rucker, C. Reddy, O. Salzman, A. Kuntz, Safer motion planning of steerable needles via a shaft-to-tissue force model. *J. Med. Rob. Res.* **08**, 2350003 (2023).
171. A. Favaro, A. Segato, F. Muretti, E. De Momi, An evolutionary-optimized surgical path planner for a programmable bevel-tip needle. *IEEE Trans. Rob.* **37**, 1039–1050 (2021).
172. A. Segato, M. Di Marzo, S. Zucchelli, S. Galvan, R. Secoli, E. De Momi, Inverse reinforcement learning intra-operative path planning for steerable needle. *IEEE Trans. Biomed. Eng.* **69**, 1995–2005 (2022).
173. S. Patil, J. van den Berg, R. Alterovitz, "Motion planning under uncertainty in highly deformable environments" in *Robotics: Science and Systems (RSS)* (RSS, 2011), pp. 1–8.
174. F. Liu, A. Garriga-Casanovas, R. Secoli, F. Rodriguez y Baena, Fast and adaptive fractal tree-based path planning for programmable bevel tip steerable needles. *IEEE Robot. Autom. Lett.* **1**, 601–608 (2016).
175. M. Pinzi, S. Galvan, F. Rodriguez y Baena, The adaptive hermite fractal tree (AHFT): A novel surgical 3D path planning approach with curvature and heading constraints. *Int. J. Comput. Assist. Radiol. Surg.* **14**, 659–670 (2019).
176. M. Fu, K. Solovey, O. Salzman, R. Alterovitz, Toward certifiable optimal motion planning for medical steerable needles. *Int. J. Rob. Res.* **42**, 798–826 (2023).
177. D. Glozman, M. Shoham, "Flexible needle steering and optimal trajectory planning for percutaneous therapies" in *Medical Image Computing and Computer Assisted Intervention (MICCAI)* (Springer, 2004), pp. 137–144.
178. C. Bergeles, A. H. Gosline, N. V. Vasilyev, P. J. Codd, P. J. Del Nido, P. E. Dupont, Concentric tube robot design and optimization based on task and anatomical constraints. *IEEE Trans. Rob.* **31**, 67–84 (2015).
179. X. Yang, S. Song, L. Liu, T. Yan, M. Q.-H. Meng, Design and optimization of concentric tube robots based on surgical tasks, anatomical constraints and follow-the-leader deployment. *IEEE Access* **7**, 173612–173625 (2019).
180. C. Baykal, C. Bowen, R. Alterovitz, Asymptotically optimal kinematic design of robots using motion planning. *Auton. Rob.* **43**, 345–357 (2019).
181. C. Girerd, T. Schlinquer, N. Andreff, P. Renaud, K. Rabenorosoa, Design of concentric tube robots using tube patterning for follow-the-leader deployment. *J. Mech. Robot.* **13**, 011006 (2021).
182. Y. Xu, C. Watson, J.-T. Lin, J. T. Hwang, T. K. Morimoto, Shape control of concentric tube robots via approximate follow-the-leader motion. *IEEE Rob. Autom. Lett.* **9**, 7198–7205 (2024).
183. J. Hoelscher, M. Fu, I. Fried, M. Emerson, T. E. Ertop, M. Rox, A. Kuntz, J. A. Akulian, R. J. Webster III, R. Alterovitz, Backward planning for a multi-stage steerable needle lung robot. *IEEE Rob. Autom. Lett.* **6**, 3987–3994 (2021).
184. J. Hoelscher, I. Fried, M. Fu, M. Patwardhan, M. Christman, J. Akulian, R. J. Webster, R. Alterovitz, "A metric for finding robust start positions for medical steerable needle automation" in *2022 IEEE/RSJ International Conference on Intelligent Robots and Systems (IROS)* (IEEE, 2022), pp. 9526–9533.
185. A. P. Kiraly, J. P. Helferty, E. A. Hoffman, G. McLennan, W. E. Higgins, Three-dimensional path planning for virtual bronchoscopy. *IEEE Trans. Med. Imaging* **23**, 1365–1379 (2004).
186. J. Rosell, A. Perez, P. Cabras, A. Rosell, "Motion planning for the virtual bronchoscopy" in *2012 IEEE International Conference on Robotics and Automation (ICRA)* (IEEE, 2012), pp. 2932–2937.
187. A. Segato, F. Calimeri, I. Testa, V. Corbetta, M. Riva, E. De Momi, A hybrid inductive learning-based and deductive reasoning-based 3-D path planning method in complex environments. *Auton. Rob.* **46**, 645–666 (2022).
188. Z. Cheng, M. Koskinopoulou, S. Bano, D. Stoyanov, T. R. Savarimuthu, L. S. Mattos, Sensing technologies for guidance during needle-based interventions. *IEEE Trans. Instrum. Meas.* **73**, 1–10 (2024).
189. P. Moreira, K. J. Boskma, S. Misra, "Towards MRI-guided flexible needle steering using fiber Bragg grating-based tip tracking" in *2017 IEEE International Conference on Robotics and Automation (ICRA)* (IEEE, 2017), pp. 4849–4854.
190. A. Donder, F. Rodriguez y Baena, Kalman-filter-based, dynamic 3-D shape reconstruction for steerable needles with fiber Bragg gratings in multicore fibers. *IEEE Trans. Rob.* **38**, 2262–2275 (2022).
191. D. A. Lezcano, I. I. Iordachita, J. S. Kim, "FBG-based shape-sensing to enable lateral deflection methods of autonomous needle insertion" in *2024 IEEE/RSJ International Conference on Intelligent Robots and Systems (IROS)* (IEEE, 2024), pp. 6977–6982.
192. M. L. Balter, A. I. Chen, T. J. Maguire, M. L. Yarmush, Adaptive kinematic control of a robotic venipuncture device based on stereo vision, ultrasound, and force guidance. *IEEE Trans. Ind. Electron.* **64**, 1626–1635 (2016).
193. G. Welch, G. Bishop, *An Introduction to the Kalman Filter* (University of North Carolina at Chapel Hill, 1995).
194. N. A. Wood, K. Shahrour, M. C. Ost, C. N. Riviere, "Needle steering system using dutycycled rotation for percutaneous kidney access" in *2010 Annual International Conference of the IEEE Engineering in Medicine and Biology* (IEEE, 2010), pp. 5432–5435.
195. K. B. Reed, V. Kallem, R. Alterovitz, K. Goldberg, A. M. Okamura, N. J. Cowan, "Integrated planning and image-guided control for planar needle steering" in *Proceedings of IEEE International Conference on Biomedical Robotics and Biomechatronics (BioRob)* (IEEE, 2008), pp. 819–824.
196. V. Kallem, N. J. Cowan, Image guidance of flexible tip-steerable needles. *IEEE Trans. Rob.* **25**, 191–196 (2009).

197. V. Kallem, "Vision-based control on lie groups with application to needle steering," thesis, Johns Hopkins University, Baltimore, MD (2008).
198. M. Emerson, J. M. Ferguson, T. E. Ertop, M. Rox, J. Granna, M. Lester, F. Maldonado, E. A. Gillaspie, R. Alterovitz, R. J. Webster, A. Kuntz, "A recurrent neural network approach to roll estimation for needle steering" in *Experimental Robotics: The 17th International Symposium* (Springer, 2021), pp. 334–342.
199. T. E. Ertop, M. Emerson, M. Rox, J. Granna, F. Maldonado, E. A. Gillaspie, M. Lester, A. Kuntz, D. C. Rucker, M. Fu, J. Hoelscher, I. Fried, R. Alterovitz, R. J. Webster III, "Steerable needle trajectory following in the lung: Torsional deadband compensation and full pose estimation with 5DOF feedback for needles passing through flexible endoscopes" in *Dynamic Systems and Control Conference* (American Society of Mechanical Engineers, 2020), 10.1115/DSCC2020-3163.
200. N. A. Patel, T. van Katwijk, G. Li, P. Moreira, W. Shang, S. Misra, G. S. Fischer, "Closed-loop asymmetric-tip needle steering under continuous intraoperative MRI guidance" in *2015 37th Annual International Conference of the IEEE Engineering in Medicine and Biology Society (EMBC)* (IEEE, 2015), pp. 4869–4874.
201. A. Mehrtash, M. Ghafoorian, G. Pernelle, A. Ziaei, F. G. Heslinga, K. Tuncali, A. Fedorov, R. Kikinis, C. M. Tempany, W. M. Wells III, P. Abolmaesumi, T. Kapur, Automatic needle segmentation and localization in MRI with 3-D convolutional neural networks: Application to MRI-targeted prostate biopsy. *IEEE Trans. Med. Imaging* **38**, 1026–1036 (2018).
202. X. Li, A. S. Young, S. S. Raman, D. S. Lu, Y.-H. Lee, T.-C. Tsao, H. H. Wu, Automatic needle tracking using mask R-CNN for MRI-guided percutaneous interventions. *Int. J. Comput. Assist. Radiol. Surg.* **15**, 1673–1684 (2020).
203. G. J. Vrooijink, M. Abayazid, S. Patil, R. Alterovitz, S. Misra, Needle path planning and steering in a three-dimensional non-static environment using two-dimensional ultrasound images. *Int. J. Rob. Res.* **33**, 1361–1374 (2014).
204. M. Abayazid, G. J. Vrooijink, S. Patil, R. Alterovitz, S. Misra, Experimental evaluation of ultrasound-guided 3D needle steering in biological tissue. *Int. J. Comput. Assist. Rad. Surg.* **9**, 931–939 (2014).
205. T. K. Adebar, A. E. Fletcher, A. M. Okamura, 3-D ultrasound-guided robotic needle steering in biological tissue. *IEEE Trans. Biomed. Eng.* **61**, 2899–2910 (2014).
206. E. Lobaton, J. Fu, L. G. Torres, R. Alterovitz, "Continuous shape estimation of continuum robots using x-ray images" in *Proceedings of IEEE International Conference on Robotics and Automation (ICRA)* (IEEE, 2013), pp. 717–724.
207. J. Sganga, D. Camarillo, "Orientation estimation of a continuum manipulator in a phantom lung" in *2017 IEEE International Conference on Robotics and Automation (ICRA)* (IEEE, 2017), pp. 2399–2405.
208. I. Fried, J. Hoelscher, J. A. Akulian, S. Pizer, R. Alterovitz, "Landmark based bronchoscope localization for needle insertion under respiratory deformation" in *IEEE/RSJ International Conference on Intelligent Robots and Systems (IROS)* (IEEE, 2023), pp. 6593–6600.
209. A. Majewicz, A. M. Okamura, "Cartesian and joint space teleoperation for nonholonomic steerable needles" in *Proceedings of IEEE World Haptics Conference (WHC)* (IEEE, 2013), pp. 395–400.
210. A. Seitel, C. J. Walsh, N. C. Hanumara, J.-A. Shepard, A. H. Slocum, H.-P. Meinzer, R. Gupta, L. Maier-Hein, "Development and evaluation of a new image-based user interface for robot-assisted needle placements with the Robopsy system" in *Medical Imaging 2009: Visualization, Image-Guided Procedures, and Modeling* (SPIE, 2009), pp. 305–313.
211. E. Matheson, R. Secoli, S. Galvan, F. Rodriguez y Baena, "Human-robot visual interface for 3D steering of a flexible, bioinspired needle for neurosurgery" in *Proceedings of IEEE/RSJ International Conference on Intelligent Robots and Systems (IROS)* (IEEE, 2019), pp. 5426–5431.
212. B. Padasdao, S. Lafreniere, M. Rabiei, Z. Batsaikhan, B. Konh, Teleoperated and automated control of a robotic tool for targeted prostate biopsy. *J. Med. Rob. Res.* **8**, 2340002 (2023).
213. M. Abayazid, C. Pacchierotti, P. Moreira, R. Alterovitz, D. Prattichizzo, S. Misra, Experimental evaluation of co-manipulated ultrasound-guided flexible needle steering. *Int. J. Med. Rob. Comput. Assist. Surg.* **12**, 219–230 (2016).
214. J. M. Romano, R. J. Webster, III, A. M. Okamura, "Teleoperation of steerable needles" in *Proceedings 2007 IEEE International Conference on Robotics and Automation (ICRA)* (IEEE, 2007), pp. 934–939.
215. W. Zarrad, P. Poignet, R. Cortesao, O. Company, "Towards teleoperated needle insertion with haptic feedback controller" in *2007 IEEE/RSJ International Conference on Intelligent Robots and Systems* (IEEE, 2007), pp. 1254–1259.
216. N. Abolhassani, R. V. Patel, Teleoperated master–slave needle insertion. *Int. J. Med. Rob. Comput Assist. Surg.* **5**, 398–405 (2009).
217. P. Moreira, L. Kuil, P. Dias, R. Borra, S. Misra, Tele-operated MRI-guided needle insertion for prostate interventions. *J. Med. Rob. Res.* **4**, 1842003 (2019).
218. J. Chevrie, A. Krupa, M. Babel, "Real-time teleoperation of flexible beveled-tip needle insertion using haptic force feedback and 3D ultrasound guidance" in *2019 International Conference on Robotics and Automation (ICRA)* (IEEE, 2019), pp. 2700–2706.
219. M. de Vries, M. Wijntjes, J. Sikorski, P. Moreira, N. J. van de Berg, J. van den Dobbelsteen, S. Misra, MR-guided HDR prostate brachytherapy with teleoperated steerable needles. *J. Rob. Surg.* **17**, 2461–2469 (2023).
220. H. Takahashi, T. Yonemura, N. Sugita, M. Mitsuishi, S. Sora, A. Morita, R. Mochizuki, "Master manipulator with higher operability designed for micro neuro surgical system" in *2008 IEEE International Conference on Robotics and Automation (ICRA)* (IEEE, 2008), pp. 3902–3907.
221. L. Marx, V. Groenhuis, S. Stramigioli, K. Niu, "Augmented-reality based digital twin to control an MR safe robot for breast biopsy: A benchmark study" in *2024 10th IEEE RAS/EMBS International Conference for Biomedical Robotics and Biomechatronics (BioRob)* (IEEE, 2024), pp. 814–819.
222. D. C. Rucker, J. Das, H. B. Gilbert, P. J. Swaney, M. I. Miga, N. Sarkar, R. J. Webster III, Sliding mode control of steerable needles. *IEEE Trans. Rob.* **29**, 1289–1299 (2013).
223. S. Patil, J. Burgner, R. J. Webster III, R. Alterovitz, Needle steering in 3-D via rapid replanning. *IEEE Trans. Rob.* **30**, 853–864 (2014).
224. W. Sun, S. Patil, R. Alterovitz, High-frequency replanning under uncertainty using parallel sampling-based motion planning. *IEEE Trans. Rob.* **31**, 104–116 (2015).
225. M. Pinzi, T. Watts, R. Secoli, S. Galvan, F. Rodriguez y Baena, Path replanning for orientation-constrained needle steering. *IEEE Trans. Biomed. Eng.* **68**, 1459–1466 (2021).
226. M. C. Bernardes, P. Moreira, L. Mareschal, C. Tempany, K. Tuncali, N. Hata, J. Tokuda, Data-driven adaptive needle insertion assist for transperineal prostate interventions. *Phys. Med. Biol.* **68**, 105016 (2023).
227. J. Van den Berg, S. Patil, R. Alterovitz, Motion planning under uncertainty using iterative local optimization in belief space. *Int. J. Rob. Res.* **31**, 1263–1278 (2012).
228. M. Neumann, J. Burgner-Kahrs, "Considerations for follow-the-leader motion of extensible tendon-driven continuum robots" in *IEEE International Conference on Robotics and Automation (ICRA)* (IEEE, 2016), pp. 917–923.
229. D. Halperin, O. Salzman, M. Sharir, "Algorithmic motion planning" in *Handbook of Discrete and Computational Geometry*, J. E. Goodman, J. O'Rourke, C. D. Tóth, Eds. (Chapman and Hall/CRC, 2017), pp. 1311–1342.
230. S. Karaman, E. Frazzoli, Sampling-based algorithms for optimal motion planning. *Int. J. Rob. Res.* **30**, 846–894 (2011).
231. A. Bacciotti, L. Rosier, *Liapunov Functions and Stability in Control Theory* (Springer Science & Business Media, 2005).
232. C. Knuth, G. Chou, N. Ozay, D. Berenson, Planning with learned dynamics: Probabilistic guarantees on safety and reachability via Lipschitz constants. *IEEE Rob. Autom. Lett.* **6**, 5129–5136 (2021).
233. D. Bresolin, L. Geretti, R. Muradore, P. Fiorini, T. Villa, Formal verification of robotic surgery tasks by reachability analysis. *Microprocess. Microsyst.* **39**, 836–842 (2015).
234. A. A. Geraldes, L. Geretti, D. Bresolin, R. Muradore, P. Fiorini, L. S. Mattos, T. Villa, Formal verification of medical CPS: A laser incision case study. *ACM Trans. Cyber-Phys. Syst.* **2**, 1–29 (2018).
235. Y. Kouskoulas, D. Renshaw, A. Platzer, P. Kazanzides, "Certifying the safe design of a virtual fixture control algorithm for a surgical robot" in *Proceedings of the 16th International Conference on Hybrid Systems: Computation and Control* (ACM, 2013), pp. 263–272.
236. H. J. Marcus, P. T. Ramirez, D. Z. Khan, H. Layard Horsfall, J. G. Hanrahan, S. C. Williams, D. J. Beard, R. Bhat, K. Catchpole, A. Cook, K. Hutchison, J. Martin, T. Melvin, D. Stoyanov, M. Rovers, N. Raison, P. Dasgupta, D. Noonan, D. Stocken, G. Sturt, A. Vanhoestenberghe, B. Vasey, P. McCulloch, The IDEAL Robotics Colloquium, The IDEAL framework for surgical robotics: Development, comparative evaluation and long-term monitoring. *Nat. Med.* **30**, 61–75 (2024).
237. N. E. Fard, R. R. Selmic, K. Khorasani, Public policy challenges, regulations, oversight, technical, and ethical considerations for autonomous systems: A survey. *IEEE Technol. Soc. Magaz.* **42**, 45–53 (2023).
238. Future of Life Institute (FLI), "EU Artificial Intelligence Act"; https://artificialintelligenceact.eu/.
239. D. Minh, H. X. Wang, Y. F. Li, T. N. Nguyen, Explainable artificial intelligence: A comprehensive review. *Artif. Intell. Rev.* **55**, 3503–3568 (2022).
240. A. Chaddad, J. Peng, J. Xu, A. Bouridane, Survey of explainable AI techniques in healthcare. *Sensors* **23**, 634 (2023).
241. A. Majewicz, S. P. Marra, M. G. van Vledder, M. Lin, M. A. Choti, D. Y. Song, A. M. Okamura, Behavior of tip-steerable needles in ex vivo and in vivo tissue. *IEEE Trans. Biomed. Eng.* **59**, 2705–2715 (2012).
242. T. B. Sheridan, Human–robot interaction: Status and challenges. *Hum. Factors* **58**, 525–532 (2016).
243. I. S. MacKenzie, *Human-Computer Interaction: An Empirical Research Perspective* (Elsevier, 2024).
244. G. Bansal, B. Nushi, E. Kamar, W. S. Lasecki, D. S. Weld, E. Horvitz, "Beyond accuracy: The role of mental models in human-AI team performance" in *Proceedings of the AAAI Conference on Human Computation and Crowdsourcing (HCOMP)* (AAAI, 2019), pp. 2–11.
245. R. W. Andrews, J. M. Lilly, D. Srivastava, K. M. Feigh, The role of shared mental models in human-AI teams: A theoretical review. *Theor. Issues Ergon. Sci.* **24**, 129–175 (2023).
246. M. Bombieri, M. Rospocher, S. P. Ponzetto, P. Fiorini, Surgicberta: A pre-trained language model for procedural surgical language. *Int. J. Data Sci. Anal.* **18**, 69–81 (2024).
247. C. F. Graetzel, A. Sheehy, D. P. Noonan, "Robotic bronchoscopy drive mode of the Auris Monarch platform" in *2019 International Conference on Robotics and Automation (ICRA)* (IEEE, 2019), pp. 3895–3901.
248. B. Konh, B. Padasdao, Z. Batsaikhan, S. Y. Ko, Integrating robot-assisted ultrasound tracking and 3D needle shape prediction for real-time tracking of the needle tip in needle steering procedures. *Int. J. Med. Robot.* **17**, e2272 (2021).

249. B. Maris, M.-C. Fiazza, M. De Piccoli, C. Tenga, L. Palladino, S. Puliatti, A. Iseppi, R. Ferrari, A. Piro, L. R. Bonetti, G. Ligabue, A. Tafuri, S. Micali, P. Fiorini, Preclinical validation of a semi-autonomous robot for transperineal prostate biopsy. *IEEE Trans. Med. Robot. Bionics* **4**, 311–322 (2022).
250. S. Miah, P. Servian, A. Patel, C. Lovegrove, L. Skelton, T. T. Shah, D. Eldred-Evans, M. Arya, H. Tam, H. U. Ahmed, M. Winkler, A prospective analysis of robotic targeted MRI-US fusion prostate biopsy using the centroid targeting approach. *J. Robot. Surg.* **14**, 69–74 (2020).
251. M. Sandahl, K. J. Sandahl, E. Marinovskij, T. F. Nielsen, K. D. Sørensen, M. Borre, B. P. Ulhøi, B. G. Pedersen, Prostate cancer detection rate of manually operated and robot-assisted in-bore magnetic resonance imaging targeted biopsy. *Eur. Urol. Open Sci.* **41**, 88–94 (2022).
252. S. Levy, S. N. Goldberg, I. Roth, M. Shochat, J. Sosna, I. Leichter, S. Flacke, Clinical evaluation of a robotic system for precise CT-guided percutaneous procedures. *Abdom. Radiol.* **46**, 5007–5016 (2021).

Acknowledgments

Funding: This research was supported in part by the US National Institutes of Health (NIH) under awards R01EB024864 and R01EB032385 and the US National Science Foundation (NSF) under awards 2008475, 2038855, and 2323096. The content is solely the responsibility of the authors and does not necessarily represent the official views of NIH or NSF. **Author contributions:** R.A., A.K., and J.H. all wrote and edited text for the manuscript. **Competing interests:** A.K. and R.A. are inventors on university-owned patents on medical robotic devices incorporating steerable instruments. J.H. declares no competing interests.

Submitted 17 September 2024
Accepted 10 June 2025
Published 9 July 2025
10.1126/scirobotics.adt1874

Medical needles in the hands of AI: Advancing toward autonomous robotic navigation

Ron Alterovitz, Janine Hoelscher, and Alan Kuntz

Sci. Robot. **10** (104), eadt1874. DOI: 10.1126/scirobotics.adt1874

Science Robotics (ISSN 2470-9476) is published by the American Association for the Advancement of Science. 1200 New York Avenue NW, Washington, DC 20005. The title *Science Robotics* is a registered trademark of AAAS.